The Msd1–Wdr8–Pkl1 complex anchors microtubule minus ends to fission yeast spindle pole bodies

Masashi Yukawa,[1,2] Chiho Ikebe,[1] and Takashi Toda[1]

[1]The Francis Crick Institute, Lincoln's Inn Fields Laboratory, London WC2A 3LY, England, UK
[2]Department of Molecular Biotechnology, Graduate School of Advanced Sciences of Matter, Hiroshima University, Higashi-Hiroshima 739-8530, Japan

The minus ends of spindle microtubules are anchored to a microtubule-organizing center. The conserved Msd1/SSX2IP proteins are localized to the spindle pole body (SPB) and the centrosome in fission yeast and humans, respectively, and play a critical role in microtubule anchoring. In this paper, we show that fission yeast Msd1 forms a ternary complex with another conserved protein, Wdr8, and the minus end–directed Pkl1/kinesin-14. Individual deletion mutants displayed the identical spindle-protrusion phenotypes. Msd1 and Wdr8 were delivered by Pkl1 to mitotic SPBs, where Pkl1 was tethered through Msd1–Wdr8. The spindle-anchoring defect imposed by *msd1/wdr8/pkl1* deletions was suppressed by a mutation of the plus end–directed Cut7/kinesin-5, which was shown to be mutual. Intriguingly, Pkl1 motor activity was not required for its anchoring role once targeted to the SPB. Therefore, spindle anchoring through Msd1–Wdr8–Pkl1 is crucial for balancing the Cut7/kinesin-5–mediated outward force at the SPB. Our analysis provides mechanistic insight into the spatiotemporal regulation of two opposing kinesins to ensure mitotic spindle bipolarity.

Introduction

Bipolar spindle assembly is central to accurate chromosome segregation during mitosis. Failure in this process results in cell death, birth defects, developmental abnormalities, and various human diseases including cancer (Wittmann et al., 2001; Gadde and Heald, 2004; Meunier and Vernos, 2012; Godinho and Pellman, 2014). The first step toward spindle assembly is microtubule nucleation from a microtubule-organizing center (MTOC; Pickett-Heaps, 1969). In most organisms, the centrosome (the spindle pole body [SPB] in fungi) plays an essential role as the primary MTOC (Brinkley, 1985; Lüders and Stearns, 2007). The γ-tubulin complex (γ-TuC) is responsible for this process in which the γ-TuC interacts with the microtubule minus end. The microtubule plus end on the other hand either captures the kinetochore on the chromosome or interacts with the plus end of other microtubules elongating from the opposite pole, thereby establishing symmetric bipolarity by forming interdigitating overlap zones.

One additional critical role of the microtubule minus end lies in the anchoring of spindle microtubules to the centrosome upon nucleation. This tethering function is needed for correct structural integrity of symmetrical bipolar spindles, focusing the spindle pole and proper kinetochore capture at the opposite plus end (Bornens, 2002; Dammermann et al., 2003). The γ-TuC is also involved in this anchoring step, but compared with recently advanced knowledge of microtubule nucleation (Kollman et al., 2011; Lin et al., 2014), our molecular understanding of the anchorage still remains limited.

A large number of microtubule-based motors and microtubule-associated proteins contribute to bipolar spindle assembly (Wittmann et al., 2001; Gadde and Heald, 2004; Meunier and Vernos, 2012), and some of them directly or indirectly interact with the γ-TuC on the spindle microtubule and/or at the centrosome/SPB (Goshima and Vale, 2005; Lecland and Lüders, 2014). Among a cohort of motor molecules (dynein and 14 kinesin subfamilies; Lawrence et al., 2004), plus end–directed kinesin-5 (Eg5/BimC) and minus end–directed kinesin-14 (HSET/KIFC1/XCTK2; HSET stands for a kinesin expressing in human spleen, embryo, and testes; Ando et al., 1994) particularly play pivotal roles in bipolar spindle formation (Sharp

Correspondence to Takashi Toda: takashi.toda@crick.ac.uk

C. Ikebe's present address is the Natural History Museum, London SW7 5BD, England, UK.

Abbreviations used in this paper: 3AT, 3-amino-1,2,4-triazole; γ-TuC, γ-tubulin complex; GBP, GFP-binding protein; MTOC, microtubule-organizing center; SPB, spindle pole body; TBZ, thiabendazole.

The Rockefeller University Press $30.00
J. Cell Biol. Vol. 209 No. 4 549–562
www.jcb.org/cgi/doi/10.1083/jcb.201412111

et al., 2000; Tanenbaum and Medema, 2010). The kinesin-5 motor comprises the sole kinesin subfamily that is essential for cell division and viability in most, if not all, organisms. Although kinesin molecules in general form dimers, kinesin-5 assembles into a bipolar tetramer configuration, thereby possessing a microtubule cross-linking activity in an antiparallel manner (Kashina et al., 1996). Plus end–directed movement at each dimerized head generates an outward pushing force onto the spindle poles (Kapitein et al., 2005). Depletion or inhibition of this motor protein by small molecule inhibitors (e.g., monastrol) prevents bipolar spindle formation and arrests cells in mitosis with unseparated spindle poles that nucleate monopolar spindles (Enos and Morris, 1990; Hagan and Yanagida, 1990; Hoyt et al., 1992; Roof et al., 1992; Heck et al., 1993; Mayer et al., 1999).

In contrast, in vitro the kinesin-14 motor generates an inward pulling force that antagonizes the outward force produced by kinesin-5 (Furuta and Toyoshima, 2008; Fink et al., 2009; Hentrich and Surrey, 2010). Consistent with these opposing properties, depletion or mutations of kinesin-14 efficiently restore bipolar spindle assembly in the absence of kinesin-5 activity in various organisms (Saunders and Hoyt, 1992; O'Connell et al., 1993; Pidoux et al., 1996; Mountain et al., 1999; Sharp et al., 1999; Tanenbaum and Medema, 2010; Salemi et al., 2013). Nonetheless, the spatiotemporal regulation of these kinesins in vivo remains to be explored.

We previously showed that the conserved fission yeast coiled-coil protein Msd1 (mitotic spindle disanchored 1) is localized specifically to the mitotic SPB (Toya et al., 2007). In the *msd1* deletion mutant, spindle microtubules assemble, yet fail to be tethered to the SPB; as a result, the minus end of spindles abnormally protrudes toward the cell tips beyond the SPBs. Msd1 physically interacts with the γ-TuC component Alp4/GCP2 (Vardy and Toda, 2000). Subsequent characterization of the human orthologue, hMsd1/SSX2IP, showed that this protein also is localized to the centrosome and interacts with the γ-TuC. Importantly, this orthologue is required for anchoring mitotic astral microtubules to the centrosome (Hori et al., 2014). Therefore, the principal role of the Msd1 family in microtubule anchoring to the spindle pole is conserved from fission yeast to humans.

Despite these advances, three critical questions remain to be answered: first, how Msd1 is recruited specifically to the mitotic SPB; second, how Msd1 anchors the minus end of spindle microtubules to the SPB; and third, why the minus end of spindles protrudes beyond the SPBs in the *msd1* mutant. In this present study, we sought to address these questions. We identified Wdr8 as a novel spindle-anchoring factor. Msd1 bound Wdr8, and, furthermore, Msd1 and Wdr8 formed a tertiary complex with kinesin-14 Pkl1 (Pidoux et al., 1996; Furuta et al., 2008), in which Msd1 acted as an adaptor. Herein, we show that Pkl1 transported Msd1–Wdr8 through the spindle microtubule toward the mitotic SPB, to which this tertiary complex anchored the minus end of microtubules. Finally, the Msd1–Wdr8–Pkl1 complex antagonized the outward pushing forces generated by Cut7/kinesin-5. We discuss the molecular mechanisms underlying the dynamic maintenance of bipolar spindles exerted by these antagonistic motors at the SPB.

Results

Mitosis-specific SPB component Wdr8 is required for anchoring the spindle microtubule

By performing a systematic localization study of uncharacterized ORFs, we previously reported *SPBC32H8.09* as a novel gene encoding a mitosis-specific SPB component (Fig. 1 A; Ikebe et al., 2011). The protein encoded by this gene contains a WD40 repeat domain and belongs to the highly conserved Wdr8/WRAP73 family (Fig. S1, A and B; Koshizuka et al., 2001; Mahmoudi et al., 2009). We designate this fission yeast protein Wdr8 hereafter.

Mitosis-specific SPB localization of Wdr8 is very similar to that of Msd1, which we previously identified as a conserved microtubule-anchoring factor (Toya et al., 2007; Hori et al., 2014). Indeed, these two proteins were colocalized during mitosis (Fig. S1 C). This finding led us to examine whether Wdr8 also played a role in the anchorage of the spindle microtubule to the SPB. For this purpose, we first examined the localization dependency between Wdr8 and Msd1. Interestingly, their localization at mitotic SPBs was interdependent, i.e., Wdr8 did not localize to mitotic SPBs in the *msd1* deletion mutant and vice versa, though Msd1 localization to the spindle microtubule was often observed in the *wdr8* deletion mutant (Fig. 1, A and B). Note that Msd1 was not localized to the kinetochores in either wild-type or *wdr8Δ* mutant cells (Fig. S1 D).

Next, we checked the interaction between Msd1 and Wdr8 by performing a yeast two-hybrid assay. As shown in Fig. 1 C, Wdr8 interacted with Msd1. As previously reported (Toya et al., 2007), Msd1 also interacted with itself and with Alp4/GCP2 (Vardy and Toda, 2000), which associated with another γ-TuC component, Alp6/GCP3. Consistent with a positive interaction between Msd1 and Alp4, in the temperature-sensitive *alp6-719* mutant, in which Alp4 dissociates from the SPB at the restrictive temperature (Vardy and Toda, 2000; Venkatram et al., 2004), Msd1 became partially delocalized from the SPB (Fig. 1 D).

Importantly, like *msd1Δ*, the *wdr8Δ* mutant exhibited protruding spindle microtubules (Fig. 1, E and F) and displayed a minichromosome loss at a high rate (Fig. 1 G). Consistent with their localization interdependency, the *msd1Δwdr8Δ* double mutant showed no additive effect on either the spindle protrusion or minichromosome loss phenotype (Fig. 1, F and G; Toya et al., 2007), suggesting that these two proteins acted in the same pathway, probably by forming a complex. To gain insight into the stoichiometry among Msd1, Wdr8, and Alp4 at the mitotic SPB, we quantified the fluorescence intensities of each GFP-tagged protein (produced under native promoters). The mean intensity of the Msd1 signal was approximately half of that of the Alp4 one, whereas it was nearly twice that of the Wdr8 signal (Fig. S1 E). This finding indicated that Alp4, Msd1, and Wdr8 were present at mitotic SPBs in a molar ratio of roughly 4:2:1. These results showed Wdr8 to be a novel spindle-anchoring factor acting in concert with Msd1. Furthermore, the results of the yeast two-hybrid assay suggested that Wdr8 interacted directly with Msd1 and indirectly with the γ-TuC.

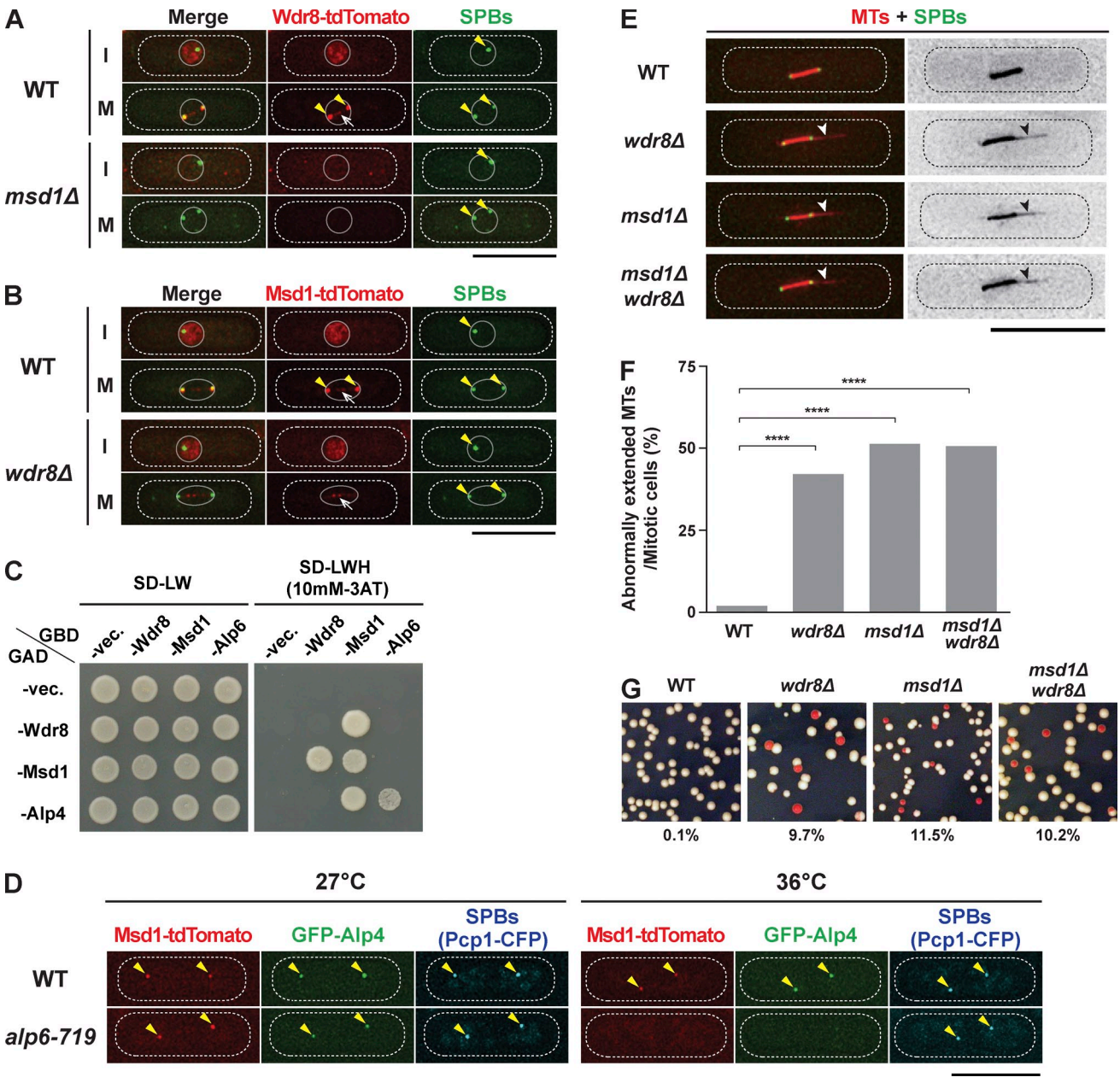

Figure 1. **Wdr8 is required for anchoring spindle microtubules to the SPB.** (A and B) Mitosis-specific SPB localization of Msd1 and Wdr8 is interdependent. Representative images of wild-type (WT) and *msd1Δ* mutant cells containing Wdr8-tdTomato and GFP-Alp4 (SPB; A) and of wild-type and *wdr8Δ* mutant cells containing Msd1-tdTomato and GFP-Alp4 (B) are shown. Localization of individual proteins during interphase (I; top) or mitosis (M; bottom) is shown in each row. Cells were grown in rich media at 27°C. The positions of SPBs and spindle microtubules are indicated with arrowheads and arrows, respectively. The peripheries of the cell and the nucleus are outlined (dotted and continuous lines, respectively). (C) Wdr8 interacts with Msd1. Yeast two-hybrid assay was performed with the indicated plasmids containing Gal4 activation domain (GAD) and Gal4 DNA-binding domain (GBD). Interaction was assessed according to growth on minimal complete synthetic defined plates lacking leucine and tryptophan (left, −LW) or leucine, tryptophan, and histidine but containing 3AT (right, −LWH, 10 mM 3AT). vec., vector. (D) Alp4 and Msd1 are delocalized from the SPB in the *alp6-719* mutant. Wild-type and *alp6-719* mutant cells containing Msd1-tdTomato, GFP-Alp4, and Pcp1-CFP, an SPB marker (Flory et al., 2002; Fong et al., 2010), were grown at 27°C (left), shifted to 36°C, and kept at that temperature for 2 h (right). Representative images of each strain are shown. The positions of SPBs are indicated with arrowheads. (E) *wdr8Δ* mutants display protruding spindle microtubules. Morphology of mitotic spindle microtubules in wild-type, *wdr8Δ*, *msd1Δ*, and *msd1Δwdr8Δ* mutant cells containing mCherry-Atb2 (microtubules [MTs]) and GFP-Alp4 (SPBs) are shown. Cells were grown in rich media at 27°C. The protrusion of spindle microtubules is indicated with arrowheads. (F) Quantification. The percentage of mitotic cells displaying abnormally extended microtubules is quantified. All p-values were obtained by performing the two-tailed χ^2 test (≥40 cells). We followed this key for asterisk placeholders for p-values in the figures: ****, $P < 0.0001$. (G) *wdr8Δ* mutants show a minichromosome loss phenotype. Indicated strains carrying the minichromosome Ch16 (Niwa et al., 1989) were grown on rich yeast extract plates (lacking adenine) and incubated at 30°C for 4 d. Cells that had lost the minichromosome formed red or red-sectored colonies. The percentages of red-sectored colonies are shown at the bottom ($n \geq 1{,}000$). Bars, 10 µm.

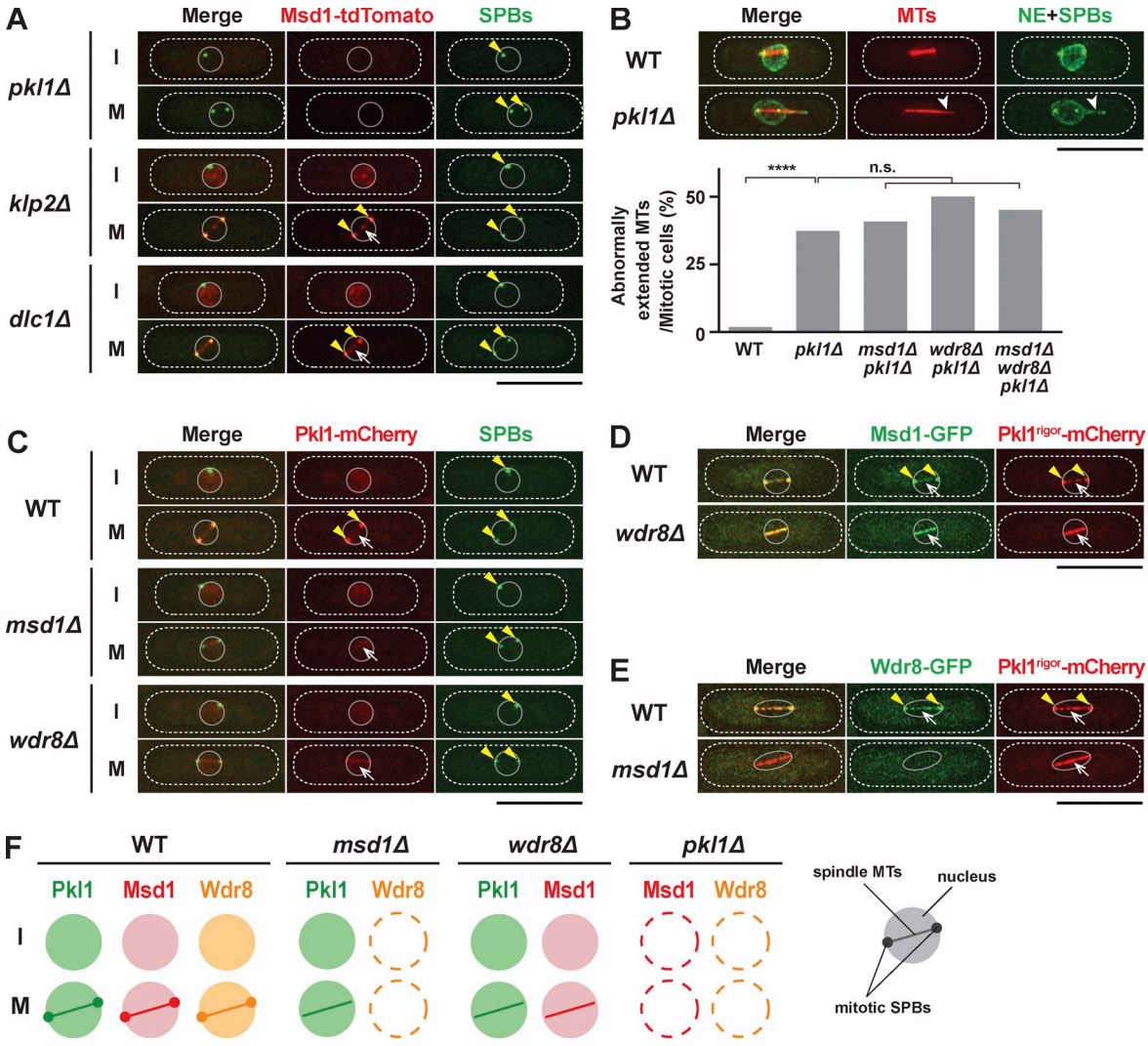

Figure 2. **Msd1 and Wdr8 act together with Pkl1/kinesin-14 for the anchorage of spindle microtubules to the SPB.** (A) SPB localization of Msd1 requires Pkl1/kinesin-14. Localization of Msd1-tdTomato and GFP-Alp4 (SPBs) in *pkl1Δ*, *klp2Δ*, or *dlc1Δ* mutant cells during interphase (I) or mitosis (M) is shown. Cells were grown in rich media at 27°C. Note that Msd1 not only is localized to the mitotic SPB (arrowheads) and spindle microtubules (arrows) but is also recognizable in the interphase nucleus in *klp2Δ* and *dlc1Δ*, but not in *pkl1Δ*, cells. (B) *pkl1Δ* mutants display protruding spindle microtubules in the nucleus. Representative images of mitotic spindle microtubules with protrusion at one end in the *pkl1Δ* mutant cells containing mCherry-Atb2 (microtubules [MTs]), GFP-Alp4 (SPBs), and Cut11-GFP (nuclear envelope [NE]; West et al., 1998) are shown. A protruding spindle microtubule is indicated with arrowheads. The percentages of cells displaying protruding spindle microtubules in various mutants are shown at the bottom. All p-values are derived from the two-tailed χ^2 test (≥40 cells; ****, $P < 0.0001$; n.s., not significant). (C) Msd1 and Wdr8 are required for Pkl1 localization to the SPBs but not to the spindle microtubules. Localization of Pkl1-mCherry and GFP-Alp4 (SPBs) in wild-type, *msd1Δ*, and *wdr8Δ* mutant cells during interphase (I) or mitosis (M) is shown. SPBs and spindle microtubules are indicated with arrowheads and arrows, respectively. (D) Msd1-GFP is colocalized with Pkl1^{rigor}-mCherry on spindle microtubules in the *wdr8Δ* mutant. SPBs and microtubules are indicated with arrowheads and arrows, respectively. (E) Wdr8-GFP is delocalized in the Pkl1^{rigor} mutant in the absence of Msd1. SPBs and spindle microtubules are indicated with arrowheads and arrows, respectively. (F) Summary of localization dependency between Msd1, Wdr8, and Pkl1. Schematic presentation of the mitotic nucleus, the SPB, and spindles is shown in the far right corner. The peripheries of the cell and the nucleus are outlined in the images (dotted and continuous lines, respectively). Bars, 10 µm.

Pkl1/kinesin-14 is required for Msd1–Wdr8 localization and the anchorage of spindle microtubules to the SPB

In addition to the circumstance in *wdr8Δ* cells (Fig. 1 B), even in wild-type cells, we often observed Msd1 localization to the spindle microtubules in between the two SPBs (Toya et al., 2007), though the signal intensities appeared to be increased in the *wdr8Δ* cells. This observation raised the possibility that Msd1 (and Wdr8) might be transported toward the SPB through the spindle microtubule. If that were the case, minus end–directed motors would be responsible. In the fission yeast genome, there are three such motors: dynein and two kinesin-14 members, Pkl1 and Klp2 (Pidoux et al., 1996; Yamamoto et al., 1999; Troxell et al., 2001). We then examined Msd1 localization at mitotic SPBs in each deletion mutant. Although Msd1 was localized normally to the mitotic SPB in either *dlc1Δ* (encoding dynein light chain; Miki et al., 2002) or *klp2Δ* cells, in the *pkl1* deletion mutant, the Msd1 signals were completely absent from both the SPB and spindle microtubules (Fig. 2 A, rows marked as M). Additionally, we noted that although Msd1

signals were observable in the whole nucleoplasm during interphase in wild-type cells (see also Fig. 1 B) as well as in *dlc1Δ* or *klp2Δ* mutants, this interphase localization was also diminished in the absence of Pkl1 (Fig. 2 A, rows marked as I). Likewise, Wdr8 also was delocalized in *pkl1Δ* mutants (Fig. S2 A). Total protein levels of Msd1 and Wdr8 did not differ between wild-type and *pkl1Δ* cells (see Fig. 3 C).

Consistent with the delocalization of Msd1 and Wdr8 from the mitotic SPB, *pkl1*-deleted cells displayed protruding spindle phenotypes exactly like those of *msd1Δ* or *wdr8Δ* (Fig. 2 B). No additive defects were observed when these genes were multiply deleted in any combinations, supporting the proposition that they functioned together in a single pathway. Previously, it was shown that the *pkl1* deletion mutant is hypersensitive to thiabendazole (TBZ), an antimicrotubule drug (Pidoux et al., 1996). We found that *msd1Δ* and *wdr8Δ* mutants were also hypersensitive to this drug and that the sensitivity of the double or triple mutants among these gene-deleted cells was not additive (Fig. S2 B).

We next addressed the requirement of the spindle microtubules for SPB localization of Msd1–Wdr8. Microtubule depolymerization experiments resulted in the disappearance of Msd1 from both SPBs (Fig. S2 C), indicating that microtubules were needed to retain Msd1 at mitotic SPBs. Furthermore, even the initial recruitment of this complex to the SPB upon mitotic entry required microtubules, as Msd1 failed to localize to the SPB in the cold-sensitive β-tubulin mutant, *nda3-KM311* (Fig. S2 D; Hiraoka et al., 1984). Collectively, these results suggest that Pkl1 transported Msd1–Wdr8 along the spindle microtubule toward mitotic SPBs.

Msd1 and Wdr8 are required for the loading of Pkl1/kinesin-14 to the mitotic SPB

As reported previously (Pidoux et al., 1996; Paluh et al., 2000), we confirmed that during mitosis Pkl1 was localized strongly to the SPBs and less prominently to the spindle microtubules (Fig. 2 C), reminiscent of localization profiles of Msd1 and Wdr8 (Fig. 1, A and B). We found that in the *msd1Δ* or *wdr8Δ* mutant, Pkl1 localization to the mitotic SPB was abolished; however, that to the spindle microtubule and interphase nucleus was still observable (Fig. 2 C). Thus, Msd1 and Wdr8 appeared to be specifically required for the loading of Pkl1 to the mitotic SPB.

To substantiate this notion, we introduced a single point mutation (G580E) within the ATP-binding domain (P-loop [phosphate-binding loop]) of Pkl1, thereby generating a rigor mutant that interacts with microtubules in a nucleotide-independent manner (Meluh and Rose, 1990; Rodriguez et al., 2008). In the *wdr8*$^{+}$ or *msd1*$^{+}$ background, Pkl1^{rigor}-mCherry and Msd1-GFP or Pkl1^{rigor}-mCherry and Wdr8-GFP, respectively, accumulated more clearly on the spindle microtubules, though the localization to mitotic SPBs was still detected (Fig. 2, D or E, respectively). In sharp contrast, in the absence of Wdr8, Msd1-GFP was colocalized with Pkl1^{rigor}-mCherry only at the spindle microtubules (Fig. 2 D). In the *msd1Δ* mutant, on the other hand, Wdr8-GFP localization was completely abolished, whereas Pkl1^{rigor}-mCherry was localized only to the mitotic spindle (Fig. 2 E). A schematic summary of protein localization patterns in the wild type and in each deletion mutant is depicted in Fig. 2 F.

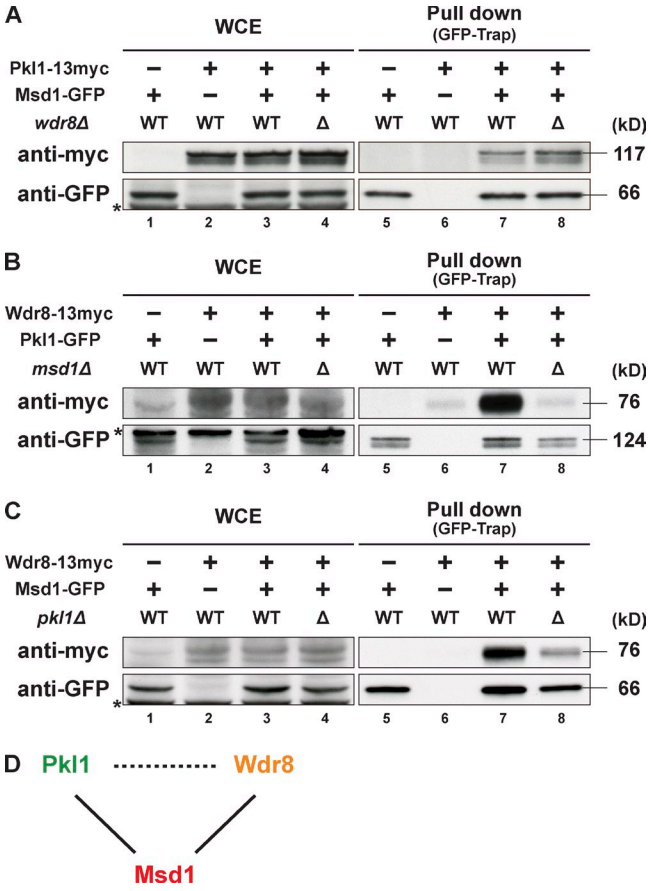

Figure 3. **Wdr8 physically interacts with Pkl1/Kinesin-14 through Msd1.** (A) Msd1 and Pkl1 interact in the presence or absence of Wdr8. Pull-down assays were performed by using the GFP-trap system. Extracts were prepared from cells containing Msd1-GFP alone (lanes 1 and 5), Pkl1-13myc alone (lanes 2 and 6), or both in *wdr8*$^{+}$ (lanes 3 and 7) and *wdr8Δ* mutant (lanes 4 and 8). Immunoblotting with anti-myc (top) or anti-GFP antibodies (bottom) against whole cell extracts (WCE; lanes 1–4) and pull-down precipitates (lanes 5–8) is shown. (B) Wdr8 interacts with Pkl1 only in the presence of Msd1. Pull-down was performed as in A by using extracts prepared from cells containing Pkl1-GFP alone (lanes 1 and 5), Wdr8-13myc alone (lanes 2 and 6), or both in *msd1*$^{+}$ (lanes 3 and 7) and *msd1Δ* mutant (lanes 4 and 8). (C) Msd1 and Wdr8 interact in the presence or absence of Pkl1. Pull-down was performed as in A by using extracts prepared from cells containing Msd1-GFP alone (lanes 1 and 5), Wdr8-13myc alone (lanes 2 and 6), or both in *pkl1*$^{+}$ (lanes 3 and 7) or *pkl1Δ* mutant (lanes 4 and 8). In A–C, asterisks denote unspecific bands. (D) Summary of physical interactions among the three proteins. Msd1 interacts with Pkl1 or Wdr8 in the absence of Wdr8 or Pkl1, respectively (solid lines). Wdr8 binds to Pkl1 only in the presence of Msd1 (dotted line). WT, wild type.

Pkl1/kinesin-14 and Wdr8 interact through Msd1

Given the yeast two-hybrid data presented earlier (Fig. 1 C), we next addressed the physical interaction of Pkl1, Msd1, and Wdr8 by performing pull-down assays using extracts prepared from wild-type and individual deletion mutant cells. As shown in Fig. 3 A, Pkl1 and Msd1 formed a complex in the wild-type cells and, interestingly, even in the absence of Wdr8. This finding is consistent with the previous result showing that Pkl1 and Msd1 were colocalized to the mitotic spindles in the *wdr8Δ* mutant (Figs. 1 B and 2, C and D). Wdr8 also bound Pkl1, but this interaction did not occur in *msd1Δ* (Fig. 3 B), again consistent with the previous data showing that Wdr8 localization was dependent

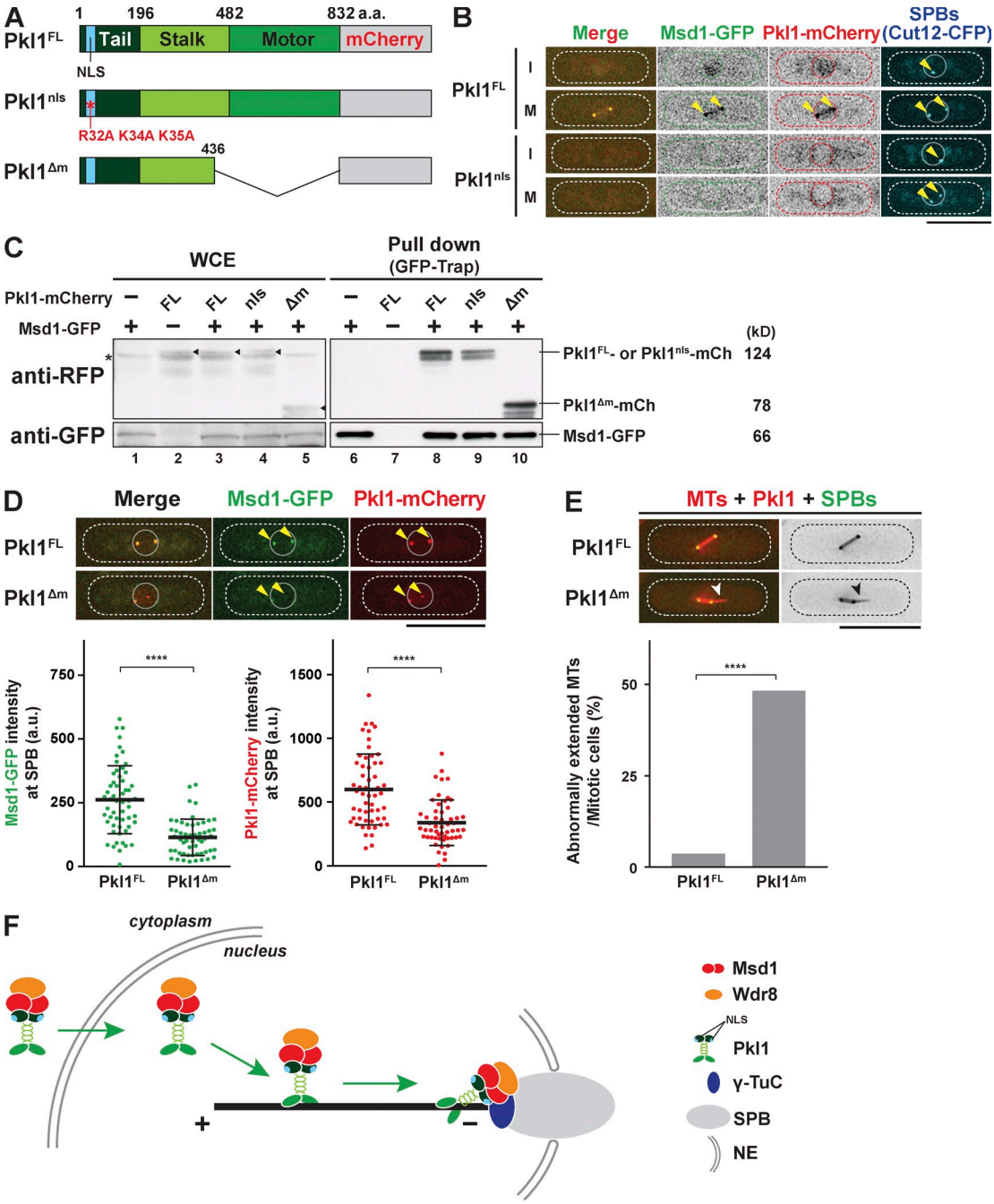

Figure 4. **Msd1 and Wdr8 are cargo proteins of Pkl1/Kinesin-14.** (A) Schematic representation of full-length Pkl1 ($Pkl1^{FL}$), an NLS mutant ($Pkl1^{nls}$), and C-terminal truncation ($Pkl1^{\Delta m}$) mutant. (B) The NLS sequence within Pkl1 is required for SPB localization of Msd1. Representative mitotic cells containing Msd1-GFP and Cut12-CFP (SPBs; Bridge et al., 1998) with $Pkl1^{FL}$-mCherry (top) or $Pkl1^{nls}$-mCherry (bottom) are shown. Each representative image of interphase (I) and mitosis (M) is presented. The positions of SPBs are indicated with arrowheads. (C) Msd1 interacts with Pkl1 that lacks NLS activity or the motor domain. Pull-down assays were performed by using the GFP-trap system, and extracts were prepared from cells containing Msd1-GFP alone (lanes 1 and 6), Pkl1-mCherry (mCh) alone (lanes 2 and 7), or both in *pkl1*$^+$ ($Pkl1^{FL}$, lanes, 3 and 8), *nls* mutant ($Pkl1^{nls}$, lanes 4 and 9), or motor-less construct ($Pkl1^{\Delta m}$, lanes 5 and 10). Immunoblotting with anti-RFP (top) or anti-GFP antibodies (bottom) is shown against whole cell extracts (WCE; lanes 1–4) and pull-down precipitates (lanes 5–8). FL, full length. (D) SPB localization of Msd1 is dependent on the motor domain of Pkl1. Representative mitotic localization of Msd1-GFP in cells containing $Pkl1^{FL}$-mCherry (top row) or motor-less $Pkl1^{\Delta m}$–mCherry (bottom row) is shown. Quantification of signal intensities of Msd1-GFP or Pkl1-mCherry at the SPB is shown at the bottom. The positions of SPBs are indicated with arrowheads. All p-values were obtained from the two-tailed unpaired Student's *t* test. Data are presented as the means ± SD (≥50 cells, $n = 3$). ****, $P < 0.0001$. a.u., arbitrary unit. (E) The motor-less Pkl1 mutant is defective in spindle anchoring. Mitotic cells containing GFP-Alp4 (SPBs), mCherry-Atb2 (microtubules [MTs]), and $Pkl1^{FL}$-mCherry (top row) or $Pkl1^{\Delta m}$-mCherry (bottom row) were fixed and imaged. The protruding spindle is indicated with arrowheads. P-value is derived from the two-tailed χ^2 test (≥50 cells; ****, $P < 0.0001$). (F) Schematic illustration of the localization scheme for Msd1, Wdr8, and Pkl1. Pkl1 forms a complex with Msd1 and Wdr8 in the cytoplasm and imports this complex into the nucleus. Upon mitotic entry and spindle formation, this complex is transported along the spindle microtubule toward the SPB, to which Msd1 and Wdr8 are responsible for loading this ternary complex through interaction with the γ-TuC. The minus end of the spindle microtubule is subsequently tethered to the SPB. NE, nuclear envelope. The peripheries of the cell and the nucleus are outlined in the images (dotted and continuous lines, respectively). Bars, 10 µm.

on Msd1 (Figs. 1 A and 2 E). On the other hand, Msd1 bound Wdr8, in the presence or absence of Pkl1 (Fig. 3 C). Overall interaction modes of Msd1, Wdr8, and Pkl1 are summarized in Fig. 3 D, which shows that these three proteins formed a ternary complex in which Msd1 acted as an adaptor for the other two proteins.

The Msd1–Wdr8 complex is cargo of the Pkl1 motor

To further investigate the mechanisms by which Msd1, Wdr8, and Pkl1 were targeted to the mitotic SPBs, we explored the physical interaction between Pkl1 and Msd1–Wdr8 in more detail. Pkl1/kinesin-14 is a minus end–directed motor (Furuta et al., 2008), in which the motor domain is found in the C-terminal half (482–832), whereas the N-terminal half consists of the tail (1–196) and stalk regions (197–481) comprising clustered coiled coils (Fig. 4 A; Troxell et al., 2001). In addition, a canonical NLS was earlier identified in its N-terminal part (29LIYRPKKIIK38; Pidoux et al., 1996; Olmsted et al., 2013). As Pkl1 together with Msd1 was localized to the nucleus during interphase (Fig. 2, A and C), we posited that this NLS sequence was responsible for nuclear localization. To scrutinize this proposition, we created point mutations (R32A, K34A, and K35A) within the NLS of Pkl1 ($Pkl1^{nls}$; Fig. 4 A), integrated $Pkl1^{nls}$ into the endogenous locus under the native promoter with mCherry in the C terminus, and examined $Pkl1^{nls}$ and Msd1 localizations. As shown in Fig. 4 B, both Msd1-GFP and $Pkl1^{nls}$-mCherry signals became delocalized from all three locations, i.e., the mitotic SPB, spindle microtubules, and the interphase nucleoplasm. Nonetheless, a pull-down experiment showed that $Pkl1^{nls}$-mCherry still interacted with Msd1-GFP (Fig. 4 C), suggesting that interaction had taken place in the cytoplasm. These data indicate that the Msd1–Wdr8–Pkl1 ternary complex was imported into the nucleus by means of the NLS situated in Pkl1.

Next, we addressed whether the motor domain of Pkl1 was required for the recruitment of Msd1 to the mitotic SPB. To this end, we generated a truncated mutant lacking this domain ($Pkl1^{\Delta m}$; Fig. 4 A). We found that the signal intensities of both Msd1-GFP and $Pkl1^{\Delta m}$-mCherry at the mitotic SPB were significantly reduced compared with those of wild-type cells (Fig. 4 D). Critically, the *pkl1*$^{\Delta m}$ mutant cells displayed the protruding spindle phenotype like the *pkl1*-null mutant (Fig. 4 E and compare with Fig. 2 B). Colocalization between Msd1-GFP and $Pkl1^{\Delta m}$-mCherry, albeit at reduced intensities at the SPB, suggested that Msd1 and motorless Pkl1 still interacted. In fact, the results of a pull-down assay confirmed this notion (Fig. 4 C). The addition of an NLS sequence (Kalderon et al., 1984) to Msd1 and Wdr8 (Msd1-NLS_{SV40}-tdTomato and Wdr8-NLS_{SV40}-tdTomato, respectively) was not sufficient for the localization of these fusion proteins to the SPB nor for the spindle anchoring function (Fig. S3, A–D), confirming that Pkl1 was essential for the delivery of Msd1–Wdr8 to the SPB. We surmise that the Msd1–Wdr8 complex was cargo of the Pkl1 motor. Together, our data suggest that Pkl1 first imported Msd1–Wdr8 from the cytoplasm to the nucleus and then delivered this cargo through the spindle microtubule to the SPB, where it was loaded on to the SPB in an Msd1- and Wdr8-dependent manner (Fig. 4 F).

Mutation of Cut7/kinesin-5 rescues the protruding phenotypes derived from the *msd1* deletion

We wondered why the minus end of microtubules was pushed out beyond the SPB in the absence of Msd1–Wdr8–Pkl1 functions and asked whether any force was responsible for this protrusion. It has been reported that in many organisms balanced opposing forces generated by kinesin-14 and kinesin-5 antagonize each other, thereby forming and maintaining the bipolar spindle architecture (Sharp et al., 2000). In fission yeast, Cut7, the sole kinesin-5, is essential for mitotic progression, bipolar spindle assembly, SPB separation, and cell viability (Hagan and Yanagida, 1990, 1992). Furthermore, the temperature sensitivity of *cut7* mutants is suppressed by the introduction of *pkl1Δ* (Pidoux et al., 1996; Troxell et al., 2001; Rodriguez et al., 2008; Olmsted et al., 2013, 2014). Intrigued by these previous findings, we next asked whether the *msd1* or *wdr8* deletion could also rescue *cut7* mutants from their temperature sensitivity. All double mutant cells containing *cut7-21msd1Δ*, *cut7-22msd1Δ*, *cut7-21wdr8Δ*, or *cut7-22wdr8Δ* could form colonies at 36°C (Figs. 5 A and S4, A and B). *cut7-22* displayed modest resistance to TBZ, and consistent with the rescue from temperature sensitivity, its TBZ resistance was likewise mitigated by *msd1Δ* or *wdr8Δ* (Fig. 5 A). Interestingly, the TBZ hypersensitivity of *msd1Δ* was reciprocally suppressed by the *cut7* mutations. Therefore, suppression of TBZ sensitivity was mutual between *msd1Δ* and *cut7-22*. Rescue of *cut7* mutants by *msd1Δ* was allele specific, as is the case for *pkl1Δ* (Pidoux et al., 1996); the most severe mutant allele, *cut7-446* (Hagan and Yanagida, 1990), failed to be ameliorated by *msd1Δ* (Fig. S4 A).

Next, we observed the spindle behavior of the *cut7-21msd1Δ* double mutant. Although most (>75%) of the *cut7-21* cells exhibited characteristic V-shaped monopolar spindle phenotypes at 36°C, as previously shown (Hagan and Yanagida, 1990), the double mutant showed a prolonged period of short spindles, which eventually elongated into full-length spindles (Fig. 5 B and Videos 1–4). Importantly, we did not detect the emergence of spindle protrusions toward the cell tips in this double mutant when it was incubated at 36°C; even at the lower temperature (27°C), the frequency of the protruding spindle microtubule phenotype in the double *cut7-21msd1Δ* mutant was substantially reduced compared with that of the *msd1Δ* single mutant (19% vs. 48%; Fig. 5 C). These data indicate that the *msd1* deletion and *cut7-21* mutation exhibited mutual suppression of spindle architecture, consistent with the data for TBZ sensitivity shown earlier (Fig. 5 A).

Cut7 accumulated at the SPB and also was localized to the spindle microtubules during mitosis (Fig. 5 D, left), as previously reported (Hagan and Yanagida, 1992; Drummond and Hagan, 1998; Fu et al., 2009). In contrast, Cut7 in the *msd1* or *pkl1* mutant displayed additional localization to the tip of protruding microtubules (Fig. 5 D, arrowheads in middle and right images). This tip corresponds to the microtubule minus end (Toya et al., 2007). However, Cut7/kinesin-5 is a plus-end motor; therefore, this tip localization appears to have been contradictory to its motility. Interestingly, though, it was shown that both budding yeast kinesin-5 Cin8 and Cut7 possess minus-end

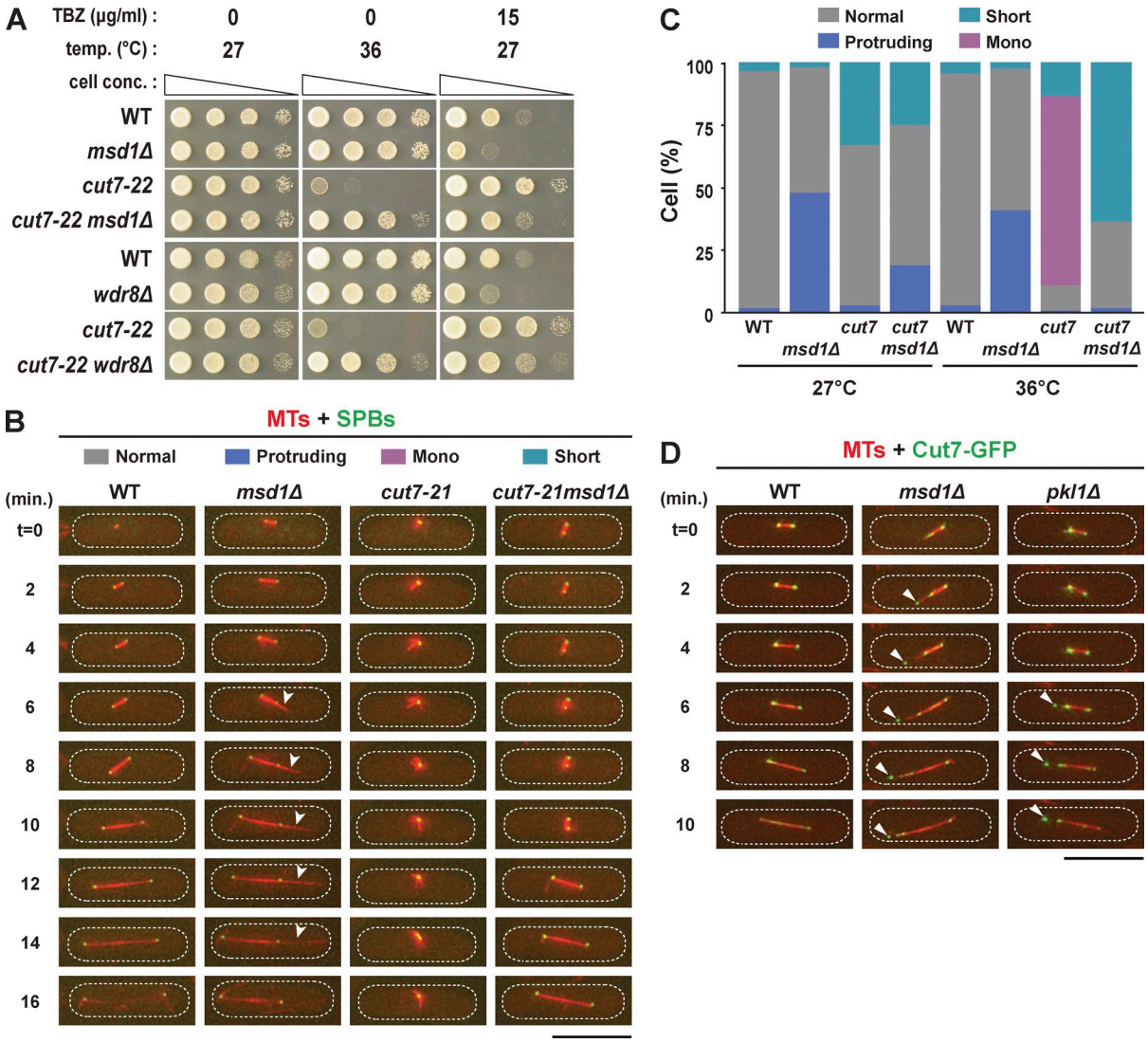

Figure 5. **Mutual suppression of defective phenotypes in double mutants between *cut7* and *msd1* or *wdr8*.** (A) Suppression of temperature and TBZ sensitivity. Serial dilution spot tests were performed by using the indicated strains on rich agar media in the presence or absence of thiabendazole (TBZ), and the cells were incubated at the indicated temperatures for 3 d. cell conc., cell concentration. (B) Time-lapse images showing mitotic progression and spindle microtubule morphology. Live imaging of individual strains that contained mCherry-Atb2 (microtubules [MTs]) and GFP-Alp4 (SPBs) was performed at 36°C. Three distinct characteristic phenotypes were identified (protruding spindles, *msd1Δ*; monopolar spindles, *cut7-21*; short spindles, *cut7-21msd1Δ*). Representative images from wild-type (Video 1), *msd1Δ* (Video 2), *cut7-21* (Video 3), and *cut7-21msd1Δ* (Video 4) cells are shown. Arrowheads show protruding spindle microtubules. (C) Quantification of phenotypes in each mutant. Cells that spent ≥10 min with short spindles (see the *cut7-21msd1Δ* cell in B) were classified as short. At least 20 mitotic cells of each strain were observed. (D) Abnormal localization of Cut7 in *msd1* or *pkl1* deletion mutants. Time-lapse imaging of Cut7-GFP and mCherry-Atb2 (microtubules) in wild-type, *msd1Δ*, and *pkl1Δ* cells is shown. Cut7-GFP signals accumulating close to the tips of the protruding spindle microtubules are marked by arrowheads in the *msd1Δ* or *pkl1Δ* mutant cell. The peripheries of the cell are outlined in the images with dotted lines. WT, wild type. Bars, 10 μm.

motility when they interact with microtubules in a nonbipolar manner (Roostalu et al., 2011; Edamatsu, 2014). We therefore surmise that Cut7's intrinsic minus-end directionality allows this molecule to be translocated toward the tip of protruding microtubules in the *msd1* or *pkl1* mutant. Hence, the results presented in this study indicate that in the absence of Msd1 or Wdr8, both Pkl1 and Cut7 became mislocalized. We conclude that excessive outward forces generated by Cut7 led to protruding spindle microtubules when Pkl1 was absent from or not properly tethered to the mitotic SPB.

Forced tethering of Pkl1 to the SPB, in either the presence or absence of its motor activity, alone fulfils its microtubule-anchoring role

Finally, we addressed whether Pkl1 served only as transport machinery for the delivery of the Msd1–Wdr8 complex to the SPB; if this were the case, when delivered, Pkl1 should no longer be necessary for spindle anchoring. To clarify this point, we adopted the GFP entrapment strategy based upon the implementation of GFP-binding protein (GBP; Rothbauer et al., 2008). We created

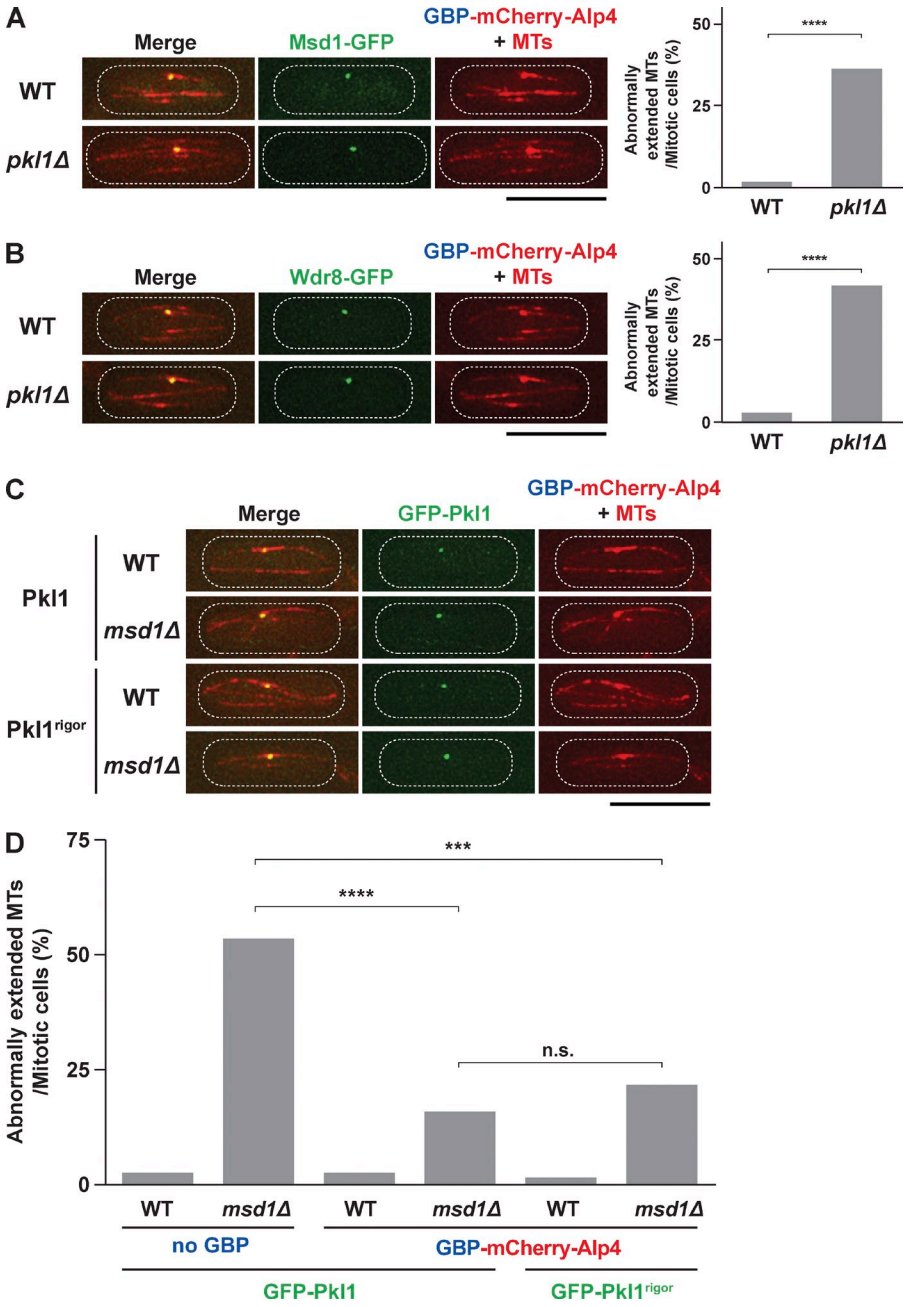

Figure 6. **Tethering of Pkl1, either wild type or the rigor mutant, to the SBP is largely sufficient for spindle anchoring.** (A) Tethering Msd1 to the SPB is not sufficient for spindle anchoring in the absence of Pkl1. Representative interphase images of Msd1-GFP, GBP-mCherry-Alp4 signals, and mCherry-Atb2 (microtubules [MTs]) in the wild-type (top) and *pkl1Δ* mutant (bottom) cells are shown. (left) Note that Msd1-GFP is colocalized with the SPB/Alp4 during interphase. Quantification of spindle-anchoring defects is shown on the right. P-value was obtained from the two-tailed χ^2 test (≥50 cells; ****, $P < 0.0001$). (B) Tethering Wdr8 to the SPB is not sufficient for spindle anchoring in the absence of Pkl1. Representative interphase images as in A are shown except that the localization of Wdr8-GFP is displayed. P-value was obtained from the two-tailed χ^2 test (≥50 cells; ****, $P < 0.0001$). (C) Tethering of Pkl1 to the SPB in wild type or *msd1Δ*. GFP-Pkl1, either wild type (top two rows) or the rigor mutant (bottom two rows), was tethered to the SPB by using GBP-mCherry-Alp4. Representative interphase images as in A are shown except that the localization of GFP-Pkl1 is displayed. (D) Tethering Pkl1, either wild type or rigor, to the SPB alone significantly rescues spindle-anchoring defects in *msd1Δ*. All p-values were obtained from the two-tailed χ^2 test (≥50 cells; ***, $P < 0.001$; ****, $P < 0.0001$; n.s., not significant). The peripheries of the cell are outlined in the images with dotted lines. WT, wild type. Bars, 10 µm.

a strain containing GBP-mCherry-Alp4 produced from the native promoter. When combined with Msd1-GFP or Wdr8-GFP, both GFP signals were now found constitutively at the SPB independent of the cell cycle stage (Fig. 6, A and B, top left), which indicated that the GFP entrapment strategy was successful. Consistently, Msd1-GFP or Wdr8-GFP was localized to the SPB in the absence of Pkl1 (Fig. 6, A and B, bottom left). Importantly, however, inspection of spindle morphologies showed that in the absence of Pkl1, the cells displayed spindle-protruding phenotypes indistinguishable from those of the simple *pkl1Δ* mutant (Fig. 6, A and B, right). This result clearly indicated that the Msd1–Wdr8 complex at the SPB was not sufficient for spindle anchoring, i.e., Pkl1 played an additional role beyond that as delivery machinery.

Next, we performed complementary tethering experiments, in which Pkl1 was targeted to the SPB in wild-type, *msd1Δ*, or *wdr8Δ* cells (Figs. 6 C and S5 A). We found that in these combinations, spindle-protruding phenotypes observed in *msd1Δ* or *wdr8Δ* were significantly, albeit partially, recovered (Figs. 6 D and S5 B). Hence, SPB localization of Pkl1 was largely enough for spindle anchoring. We further explored whether the motor activity of Pkl1 was necessary for the anchoring role by using the rigor mutant. Intriguingly, GFP-Pkl1^{rigor} also rescued the protruding spindle phenotypes in the *msd1Δ* background nearly as efficiently as did wild-type Pkl1 (Figs. 6, C and D). This result led to the notion that Pkl1 could protect spindle integrity against protrusion independent of its motor activity, provided that it was localized to the SPB. Taking these results together, we propose that spindle anchoring comprises multiple processes, including Pkl1-dependent transport

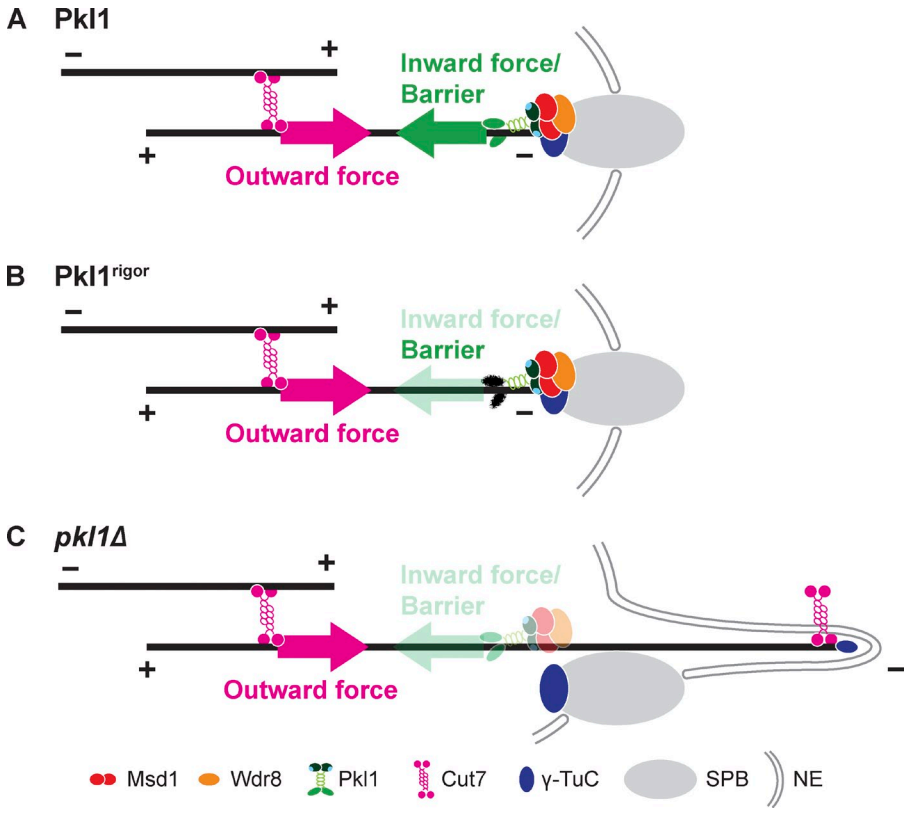

Figure 7. **A schematic model for spindle anchoring to the mitotic SPB.** (A) A model for spindle anchoring in wild-type cells. The minus end of the spindle microtubule is anchored properly to the SPB through binding between Msd1 and the γ-TuC. For this stable binding, interaction of Wdr8 with Msd1 is essential. At the SPB, inward forces generated by Pkl1/kinesin-14 within a ternary complex containing Msd1 and Wdr8 are antagonized by opposing outward forces generated by Cut7/kinesin-5 localized to the nearby overlapping microtubule zones. The Msd1–Wdr8–Pkl1 complex may play an additional, parallel role at the SPB by acting as a physical barrier resisting the Cut7/kinesin-5–mediated force. For simplicity, another separating SPB is not depicted. (B) If the nonmotile Pkl1 rigor mutant is tethered to the SPB, Pkl1^{rigor} is enough for the spindle-anchoring role as the physical barrier against Cut7/kinesin-5–mediated outward forces even in the absence of Msd1 or Wdr8. (C) Protrusion of the spindle microtubules in the absence of Pkl1 (also in the *msd1Δ* or *wdr8Δ* deletion). In the absence of the ternary complex, Cut7/kinesin-5–driven outward forces induce the protrusion of the minus end of the spindle microtubule beyond the SPB. Cut7 and occasionally the γ-TuC (Toya et al., 2007) are localized to this protruding microtubule minus end. NE, nuclear envelope.

of the Msd1–Wdr8 complex and subsequent tethering of Pkl1/kinesin-14 to the SPB by Msd1–Wdr8, which antagonizes an outward pushing force exerted by Cut7/kinesin-5.

Discussion

This study has provided mechanistic insights into how the minus end of the spindle microtubule is anchored to the SPB. First, we found that the conserved fission yeast Wdr8 protein was important for proper spindle anchoring by forming a complex with Msd1. We then showed that Pkl1/kinesin-14 bound Msd1–Wdr8 through Msd1 and imported this complex from the cytoplasm into the nucleus. Inside the nucleus, Pkl1 delivered it to the minus end of spindle microtubules, where the Msd1–Wdr8 complex associated with the γ-TuC and accordingly tethered Pkl1 to the SPB. GBP-GFP entrapping experiments strongly suggested that an inward force toward the spindle midzone and/or motor-independent barrier activity at the SPB exerted by Pkl1 was largely sufficient for proper spindle anchoring. This Pkl1-mediated mechanism in turn was fine-tuned by the counteracting Cut7/kinesin-5–dependent outward force (depicted in Fig. 7, A and B); the loss of Pkl1 from the SPB led to an unbalanced outward force imposed by Cut7, resulting in spindle protrusion (Fig. 7 C). As far as we are aware, our work is the first to identify the molecular pathway that ensures spindle anchoring to the spindle pole, which is established by proper kinesin-14 localization.

Pkl1/kinesin-14 ensures spindle anchoring to the SPB

It was previously reported that Pkl1 directly binds γ-tubulin (Rodriguez et al., 2008; Olmsted et al., 2013, 2014). However, SPB localization of Pkl1 during mitosis absolutely required the Msd1 and Pkl1 complex, suggesting that the interaction between Pkl1 and γ-tubulin played rather an auxiliary role in targeting to and/or maintaining it at the SPB. It has also been proposed that the release of γ-tubulin from the SPB through its interaction with Pkl1 impairs proper spindle formation at the step of microtubule nucleation, and Cut7 serves a function in antagonistically regulating this reaction (Olmsted et al., 2013, 2014). The data presented in this study have provided an alternative scenario, albeit not a mutually exclusive one, in which the proper force balance between Pkl1/kinesin-14 and Cut7/kinesin-5 upon microtubule nucleation is also critical for proper spindle formation. It is noteworthy that several previous studies reported the mitotic phenotypes of the *pkl1* deletion mutant, including TBZ hypersensitivity and chromosome missegregation, but the precise defects in spindle microtubule structures imposed by the absence of Pkl1 remained unnoticed (Pidoux et al., 1996; Troxell et al., 2001; Rodriguez et al., 2008). One exception was a study using EM tomography (Grishchuk et al., 2007), which unveiled abnormal organization of spindles emanating from the SPB in the *pkl1* mutant, results consistent with and complementary to our current ones.

The GBP-GFP entrapment experiments showed that tethering Pkl1 to the mitotic SPB through Alp4/γ-TuC was largely sufficient for spindle anchoring in the absence of Msd1. Furthermore, nonmotile Pkl1^{rigor} could play a substitute role, suggesting that in addition to motor activity, Pkl1 functioned as the physical barrier at the SPB by which it antagonized the Cut7/kinesin-5–mediated outward force (Fig. 7 B). However, given only the partial suppression, we surmise that

the Msd1–Wdr8 complex at the SPB served additional functions in spindle anchoring in corroboration with Pkl1, perhaps involving potentiation of Pkl1 motor activities by this complex, securing of the tight association between the microtubule minus end and the γ-TuC and/or clamping of the γ-TuC to the SPB. These functions would help ensure the localization of the minus end of the spindle microtubule to the MTOC. Further biochemical approaches will be required to explore these propositions. It is also noteworthy that the phenotypic appearance of spindle protrusion in *msd1/wdr8/pkl1* mutants was always incomplete, ∼50% penetrance, implying the existence of alternate pathways involved in spindle anchoring at the SPB.

Although spindle protrusion defects analogous to those in fission yeast have not been reported upon depletion or inactivation of animal kinesin-14 molecules, we envision that this is perhaps attributable to the presence of the dense astral microtubules emanating from the pole toward the cell cortex in animal cells, which presence would impede the visualization of protruding spindles. Alternatively, the known defects in spindle pole focusing caused by kinesin-14 knockdown (Walczak et al., 1998; Kwon et al., 2008) might represent spindle defects functionally analogous to the anchorage failure in fission yeast. It is possible that unlike yeast cells, which undergo a closed mitosis with a structurally rigid SPB embedded in the nuclear membrane, animal cells, which undergo an open mitosis, contain a mesh-like pericentriolar material (Mennella et al., 2014), which may be prone to spatial disorganization when excess pushing forces are exerted.

Spatiotemporal control and antagonism between kinesin-14 and kinesin-5

An antagonistic relationship between kinesin-14 and kinesin-5 is deemed to be well established in many organisms including fungi, flies, and humans; several genetic and cell biology studies have validated this notion (Saunders and Hoyt, 1992; O'Connell et al., 1993; Pidoux et al., 1996; Saunders et al., 1997; Mountain et al., 1999; Sharp et al., 1999, 2000; Salemi et al., 2013). This view has also been nicely substantiated by in vitro and in silico work (Walczak et al., 1998; Tao et al., 2006; Civelekoglu-Scholey et al., 2010; Hentrich and Surrey, 2010). However, the important question as to where kinesin-14 plays its critical role in vivo has not been rigorously addressed, though both human HSET and fly Ncd are localized to the spindle pole as well as to the spindle microtubules (Endow and Komma, 1996; Mountain et al., 1999; Cytrynbaum et al., 2005; Goshima and Vale, 2005). It is worth noting that human HSET, when expressed in fission yeast, is capable of localizing to the mitotic SPB and, remarkably, functionally replacing Pkl1 (Olmsted et al., 2013). This raises an intriguing possibility that HSET interacts with Msd1 and, furthermore, that pole tethering of HSET is also essential in human cells.

Conserved Msd1/SSX2IP and Wdr8/WRAP73 proteins

Both Msd1 and Wdr8 are highly conserved proteins across a wide range of eukaryotic species. Further to this structural conservation, it is known that not only does human Msd1/SSX2IP localize to the centrosome (and the basal body; Bärenz et al., 2013; Hori et al., 2014; Klinger et al., 2014), but Wdr8/WRAP73 is also a component of the centrosome (Hutchins et al., 2010; Ikebe et al., 2011; Jakobsen et al., 2011). Intriguingly, in *Aspergillus nidulans*, the only organism in which the role of Wdr8 homologues has been studied, An-WDR8 forms a complex with Msd1 (called TINA), and the localization of these two proteins to the mitotic SPB are interdependent. Importantly, TINA and An-WDR8 are essential for spindle anchoring (Osmani et al., 2003; Shen and Osmani, 2013). These results suggest that Msd1 and Wdr8 have been conserved not only structurally but also functionally. In fact, we found that human Wdr8/WRAP73 interacted with Msd1/SSX2IP (unpublished data). Whether Msd1/SSX2IP and Wdr8/WRAP73 associate with human kinesin-14 HSET is not known, nor do we know whether these two proteins are required for HSET functions. These questions need to be answered in future studies to understand in greater detail the conserved roles of the Msd1–Wdr8 complex.

Materials and methods

Strains, media, and genetic methods

Fission yeast strains used in this study are listed in Table S1. Cells were grown under standard conditions as previously described (Moreno et al., 1991). For most of the experiments, rich YE5S plates and media were used, and yeast extract plates were used for the minichromosome loss assay (Niwa et al., 1989). Wild-type strain (513; Table S1), temperature-sensitive *cut7* (*cut7-21*, *-22*, and *-446*), *pkl1* deletion, and minichromosome-containing strains were provided by P. Nurse (The Francis Crick Institute, London, England, UK), I. Hagan (Cancer Research UK Manchester Institute, University of Manchester, Manchester, England, UK), R. McIntosh (University of Colorado, Boulder, CO), and O. Niwa (Kazusa DNA Research Institute, Chiba, Japan), respectively. Spot assays were performed by spotting 5–10 µl of cells at a concentration of 2×10^7 cells/ml after 10-fold serial dilutions onto rich YE5S plates with or without a drug (TBZ). The plates were incubated at various temperatures from 25°C to 37°C as necessary.

Preparation and manipulation of nucleic acids

Enzymes were used as recommended by the suppliers (New England Biolabs, Inc. and Takara Bio Inc.).

Strain construction, gene disruption, and the N-terminal and C-terminal epitope tagging

A PCR-based gene-targeting method (Bähler et al., 1998b; Sato et al., 2005) was used for complete gene disruption and epitope tagging (e.g., GFP, tdTomato, mCherry, and 13myc) in the C terminus, by which all the tagged proteins were produced under the endogenous promoter. A strain containing GFP-Pkl1 was constructed as follows: DNA fragments containing a G418-resistance gene (*kan*), the *alp4*$^+$ promoter, and GFP (Masuda et al., 2013) were PCR amplified and inserted in frame 5′ to the *pkl1*$^+$ ORF by the fusion PCR method. Msd1-NLS$_{SV40}$-tdTomato or Wdr8-NLS$_{SV40}$-tdTomato was constructed by inserting in frame a canonical NLS sequence (PKKKRKV) derived from SV40 (Kalderon et al., 1984) 5′ to tdTomato.

The GBP-GFP protein tethering system in fission yeast

A series of plasmids, containing GBP or GBP-mCherry, was constructed in standard pFA6a-MX6 vectors that carry various drug marker genes, including *kan*, *hph*, and *nat* (Bähler et al., 1998b; Sato et al., 2005). These plasmids were used for strain constructions to perform GFP entrapment experiments by GBP (Rothbauer et al., 2008). A strain containing GBP-mCherry-Alp4 was constructed as follows. DNA fragments containing a G418-resistance gene (*kan*), the *alp4*$^+$ promoter, GBP, and mCherry were PCR amplified and inserted in frame 5′ to the *alp4*$^+$ ORF by the fusion PCR method. A plasmid containing the *GBP* sequence encoding a GFP-binding nanobody (Rothbauer et al., 2008) was a gift from H. Leonhardt (Ludwig Maximilians Munich, Department of Biology II, Planegg-Martinsried, Germany)

and G. Pereira (German Cancer Research Center [DKFZ], DKFZ–Center for Molecular Biology Alliance, Heidelberg, Germany).

Yeast two-hybrid method

Standard methods were followed as described previously (Sato et al., 2005). The budding yeast strain L40 was used as a host. Entire ORFs of interest were amplified by PCR and subcloned into corresponding vectors. Positive interactions were assessed on minimal complete synthetic defined plates lacking leucine, tryptophan, and histidine but containing 10 mM 3-amino-1,2,4-triazole (3AT).

Microtubule depolymerization experiments

Two methods were exploited. One was cold treatment. Exponentially growing cells containing Msd1-tdTomato, GFP-Alp4, and CFP-Atb2 were incubated on ice for 30 min. The same area of microscopy fields was observed before and after the cold treatment. In the other method, we used a cold-sensitive β-tubulin mutant, *nda3-KM311* (Hiraoka et al., 1984), which contained Plo1-GFP and Msd1-tdTomato. After a 6-h incubation at 19°C, a majority (>80%) of the cells were arrested in early mitosis, which could be recognized by a single Plo1-GFP dot at the SPB (Bähler et al., 1998a; Mulvihill et al., 1999). To assure complete microtubule depolymerization, we paced the *nda3-KM311* cells on ice for 10 min before observation.

Fluorescence microscopy and time-lapse live-cell imaging

Fluorescence microscopy images were obtained by using the microscope system (DeltaVision; Applied Precision) comprising a wide-field inverted epifluorescence microscope (IX71; Olympus), a Plan Apochromat 60×, NA 1.4, oil immersion objective (Olympus). DeltaVision image acquisition software (softWoRx 3.3.0; Applied Precision) equipped with a charge-coupled device camera (CoolSNAP HQ; Photometrics) was used. Live cells were imaged in a glass-bottomed culture dish (MatTek Corporation) coated with soybean lectin and incubated at 27°C for most of the strains or at 36°C for the temperature-sensitive mutants. The latter were cultured in rich YE5S media until mid–log phase at 27°C and subsequently shifted to the restrictive temperature of 36°C before observation. To keep cultures at the proper temperature, a temperature-controlled chamber (Precision Control) was used. The sections of images at each time point were compressed into a 2D projection using the DeltaVision maximum intensity algorithm. Deconvolution was applied before the 2D projection. Images were taken as 10–14 sections along the z axis at 0.3-µm intervals; they were then deconvolved and merged into a single projection. Captured images were processed with Photoshop CS5 (version 12.0; Adobe).

Quantification of fluorescent signal intensities

For quantification of signals intensities of fluorescent marker-tagged proteins (GFP-Alp4, Msd1-GFP, Wdr8-GFP, $Pkl1^{FL}$-mCherry, $Pkl1^{\Delta m}$-mCherry, Msd1-NLS_{SV40}-tdTomato, and Wdr8-NLS_{SV40}-tdTomato) located at the SPB, 10–14 sections were taken along the z-axis at 0.3-µm intervals. After deconvolution, projection images of maximum intensity were obtained, and after subtracting background intensities, values of maximum fluorescence intensities were used for statistical data analysis.

Immunochemistry

Protein extracts were prepared by mechanical disruption of cells in an extraction buffer (50 mM Tris-HCl, pH 7.4, 1 mM EDTA, 150 mM NaCl, 0.05% NP-40, 10% glycerol, 1.5 mM *p*-nitrophenyl phosphate, 1 mM phenylmethylsulfonyl fluoride, and protease inhibitor cocktail obtained from Sigma-Aldrich) with acid-washed glass beads in the FastPrep FP120 apparatus (2 × 25 s, power 5.5; BIO-101, Inc.). Extracts were cleared of debris by centrifugation for 1 min and subsequently for 5 min at 13,000 *g*. Protein concentrations were determined with a Bradford assay kit (Bio-Rad Laboratories, Inc.). A range of 3–10 mg protein was used per pull-down experiment, in which extracts were mixed with GFP-Trap, which is GBP coupled to magnetic particles (ChromoTek) and rotated for 1.5 h. The beads were then washed with wash buffer (protein extraction buffer without 1 mM dithiothreitol) and boiled in Laemmli buffer for 5 min. Protein extracts were loaded and resolved on denaturing 4–12% gradient gels (Bio-Rad Laboratories, Inc.) and transferred onto polyvinylidene fluoride membranes. The membranes were blocked with 10% skim milk and then blotted with either anti-GFP (rabbit polyclonal, TP401; Torrey Pines Biolabs), anti-RFP (rabbit polyclonal, 600-401-379; Rockland Immunochemicals), or anti-Myc (mouse monoclonal, 9E10; Covance) antibodies at a dilution of 1:1,000 in 1% skim milk. After having been washed, the blots were incubated with anti–rabbit or anti–mouse horseradish peroxidase–conjugated secondary antibody (GE Healthcare) in 1% skim milk at a dilution of 1:2,000. The ECL chemiluminescence kit (GE Healthcare) was used for detection.

Statistical data analysis

We used the two-tailed χ^2 test to evaluate the significance of differences between frequencies of mitotic cells displaying abnormally extended microtubules in different strains (Figs. 1 F; 2 B; 4 E; 6, A, B, and D; S3 D; and S5 B). For testing the significance of differences between the mean fluorescence signal intensities derived from different strains, we performed the two-tailed unpaired Student's *t* test (Figs. 4 D, S1 E, and S3 C). All the experiments were performed at least twice. Experiment sample numbers used for statistical testing were given in the corresponding figures. We used this key for asterisk placeholders to indicate p-values in the figures: e.g., ****, $P < 0.0001$.

Online supplemental material

Fig. S1 shows that Msd1 and Wdr8 are highly conserved proteins and colocalize during mitosis but do not localize to the kinetochore. Fig. S2 shows further cell biological and genetic analysis of Msd1, Wdr8, and Pkl1 as well as the dependency of SPB localization of Msd1 on the spindle microtubule. Fig. S3 shows that nuclear import of Msd1 and Wdr8 was not sufficient for their localization to the SPB or spindle anchoring in the absence of Pkl1. Fig. S4 shows that *msd1Δ* or *wdr8Δ* suppressed the temperature sensitivity of the *cut7* mutants in an allele-specific manner. Fig. S5 shows that forced tethering of Pkl1 to the SPB suppressed the spindle-protruding phenotypes in the *wdr8Δ* mutant. Table S1 shows a list of fission yeast strains used in this study. Videos 1 shows time-lapse mitotic profiles of a wild-type cell containing GFP-Alp4 (SPB) and mCherry-Atb2 (microtubule). Video 2 shows time-lapse mitotic profiles of an *msd1Δ* cell containing GFP-Alp4 (SPB) and mCherry-Atb2 (microtubule). Video 3 shows time-lapse mitotic profiles of a *cut7-21* cell containing GFP-Alp4 (SPB) and mCherry-Atb2 (microtubule). Video 4 shows time-lapse mitotic profiles of a *cut7-21msd1Δ* cell containing GFP-Alp4 (SPB) and mCherry-Atb2 (microtubule). Online supplemental material is available at http://www.jcb.org/cgi/content/full/jcb.201412111/DC1. Additional data are available in the JCB DataViewer at http://dx.doi.org/10.1083/jcb.201412111.dv.

We thank Iain Hagan, Heinrich Leonhardt, J. Richard McIntosh, Osami Niwa, Paul Nurse, and Gislene Pereira for providing materials used in this study. T. Toda and M. Yukawa express special thanks to Dai Hirata, Masaru Ueno, and Eiko Tsuchiya for their continuous support and encouragement. We are grateful to Risa Mori for useful suggestions.

M. Yukawa was supported by the Strategic Young Researcher Overseas Visits Program for Accelerating Brain Circulation from the Japan Society for the Promotion of Science. This research was supported by Cancer Research UK (T. Toda). Note that The Francis Crick Institute is a consortium of six of the UK's scientific academic organizations—the Medical Research Council (National Institute for Medical Research), Cancer Research UK (London Research Institute), the Wellcome Trust, University College London, Imperial College London, and King's College London—founded on April 1, 2015.

The authors declare no competing financial interests.

Author contributions: The experiments were designed by M. Yukawa and T. Toda. M. Yukawa performed the majority of the experiments and data analysis. C. Ikebe contributed to the initial part of this work, constructed some of the strains used, and provided the data shown in Figs. 1 (C and G) and S1 C. M. Yukawa and T. Toda wrote the paper with suggestions from C. Ikebe.

Submitted: 22 December 2014
Accepted: 16 April 2015

References

Ando, A., Y.Y. Kikuti, H. Kawata, N. Okamoto, T. Imai, T. Eki, K. Yokoyama, E. Soeda, T. Ikemura, K. Abe, et al. 1994. Cloning of a new kinesin-related gene located at the centromeric end of the human MHC region. *Immunogenetics*. 39:194–200. http://dx.doi.org/10.1007/BF00241260

Bähler, J., A.B. Steever, S. Wheatley, Y. Wang, J.R. Pringle, K.L. Gould, and D. McCollum. 1998a. Role of polo kinase and Mid1p in determining the site of cell division in fission yeast. *J. Cell Biol.* 143:1603–1616. http://dx.doi.org/10.1083/jcb.143.6.1603

Bähler, J., J.Q. Wu, M.S. Longtine, N.G. Shah, A. McKenzie III, A.B. Steever, A. Wach, P. Philippsen, and J.R. Pringle. 1998b. Heterologous modules for efficient and versatile PCR-based gene targeting in *Schizosaccharomyces pombe*. *Yeast*. 14:943–951. http://dx.doi.org/10.1002/(SICI)1097-0061(199807)14:10<943::AID-YEA292>3.0.CO;2-Y

Bärenz, F., D. Inoue, H. Yokoyama, J. Tegha-Dunghu, S. Freiss, S. Draeger, D. Mayilo, I. Cado, S. Merker, M. Klinger, et al. 2013. The centriolar satellite protein SSX2IP promotes centrosome maturation. *J. Cell Biol.* 202:81–95. http://dx.doi.org/10.1083/jcb.201302122

Bornens, M. 2002. Centrosome composition and microtubule anchoring mechanisms. *Curr. Opin. Cell Biol.* 14:25–34. http://dx.doi.org/10.1016/S0955-0674(01)00290-3

Bridge, A.J., M. Morphew, R. Bartlett, and I.M. Hagan. 1998. The fission yeast SPB component Cut12 links bipolar spindle formation to mitotic control. *Genes Dev.* 12:927–942. http://dx.doi.org/10.1101/gad.12.7.927

Brinkley, B.R. 1985. Microtubule organizing centers. *Annu. Rev. Cell Biol.* 1:145–172. http://dx.doi.org/10.1146/annurev.cb.01.110185.001045

Civelekoglu-Scholey, G., L. Tao, I. Brust-Mascher, R. Wollman, and J.M. Scholey. 2010. Prometaphase spindle maintenance by an antagonistic motor-dependent force balance made robust by a disassembling lamin-B envelope. *J. Cell Biol.* 188:49–68. http://dx.doi.org/10.1083/jcb.200908150

Cytrynbaum, E.N., P. Sommi, I. Brust-Mascher, J.M. Scholey, and A. Mogilner. 2005. Early spindle assembly in *Drosophila* embryos: role of a force balance involving cytoskeletal dynamics and nuclear mechanics. *Mol. Biol. Cell.* 16:4967–4981. http://dx.doi.org/10.1091/mbc.E05-02-0154

Dammermann, A., A. Desai, and K. Oegema. 2003. The minus end in sight. *Curr. Biol.* 13:R614–R624. http://dx.doi.org/10.1016/S0960-9822(03)00530-X

Drummond, D.R., and I.M. Hagan. 1998. Mutations in the bimC box of Cut7 indicate divergence of regulation within the bimC family of kinesin related proteins. *J. Cell Sci.* 111:853–865.

Edamatsu, M. 2014. Bidirectional motility of the fission yeast kinesin-5, Cut7. *Biochem. Biophys. Res. Commun.* 446:231–234. http://dx.doi.org/10.1016/j.bbrc.2014.02.106

Endow, S.A., and D.J. Komma. 1996. Centrosome and spindle function of the *Drosophila* Ncd microtubule motor visualized in live embryos using Ncd-GFP fusion proteins. *J. Cell Sci.* 109:2429–2442.

Enos, A.P., and N.R. Morris. 1990. Mutation of a gene that encodes a kinesin-like protein blocks nuclear division in *A. nidulans*. *Cell*. 60:1019–1027. http://dx.doi.org/10.1016/0092-8674(90)90350-N

Fink, G., L. Hajdo, K.J. Skowronek, C. Reuther, A.A. Kasprzak, and S. Diez. 2009. The mitotic kinesin-14 Ncd drives directional microtubule-microtubule sliding. *Nat. Cell Biol.* 11:717–723. http://dx.doi.org/10.1038/ncb1877

Flory, M.R., M. Morphew, J.D. Joseph, A.R. Means, and T.N. Davis. 2002. Pcp1p, an Spc110p-related calmodulin target at the centrosome of the fission yeast *Schizosaccharomyces pombe*. *Cell Growth Differ.* 13:47–58.

Fong, C.S., M. Sato, and T. Toda. 2010. Fission yeast Pcp1 links polo kinase-mediated mitotic entry to γ-tubulin-dependent spindle formation. *EMBO J.* 29:120–130. http://dx.doi.org/10.1038/emboj.2009.331

Fu, C., J.J. Ward, I. Loiodice, G. Velve-Casquillas, F.J. Nedelec, and P.T. Tran. 2009. Phospho-regulated interaction between kinesin-6 Klp9p and microtubule bundler Ase1p promotes spindle elongation. *Dev. Cell*. 17:257–267. http://dx.doi.org/10.1016/j.devcel.2009.06.012

Furuta, K., and Y.Y. Toyoshima. 2008. Minus-end-directed motor Ncd exhibits processive movement that is enhanced by microtubule bundling in vitro. *Curr. Biol.* 18:152–157. http://dx.doi.org/10.1016/j.cub.2007.12.056

Furuta, K., M. Edamatsu, Y. Maeda, and Y.Y. Toyoshima. 2008. Diffusion and directed movement: in vitro motile properties of fission yeast kinesin-14 Pkl1. *J. Biol. Chem.* 283:36465–36473. http://dx.doi.org/10.1074/jbc.M803730200

Gadde, S., and R. Heald. 2004. Mechanisms and molecules of the mitotic spindle. *Curr. Biol.* 14:R797–R805. http://dx.doi.org/10.1016/j.cub.2004.09.021

Godinho, S.A., and D. Pellman. 2014. Causes and consequences of centrosome abnormalities in cancer. *Philos. Trans. R. Soc. Lond. B Biol. Sci.* 369:20130467. http://dx.doi.org/10.1098/rstb.2013.0467

Goshima, G., and R.D. Vale. 2005. Cell cycle-dependent dynamics and regulation of mitotic kinesins in *Drosophila* S2 cells. *Mol. Biol. Cell*. 16:3896–3907. http://dx.doi.org/10.1091/mbc.E05-02-0118

Grishchuk, E.L., I.S. Spiridonov, and J.R. McIntosh. 2007. Mitotic chromosome biorientation in fission yeast is enhanced by dynein and a minus-end-directed, kinesin-like protein. *Mol. Biol. Cell*. 18:2216–2225. http://dx.doi.org/10.1091/mbc.E06-11-0987

Hagan, I., and M. Yanagida. 1990. Novel potential mitotic motor protein encoded by the fission yeast *cut7*$^{+}$ gene. *Nature*. 347:563–566. http://dx.doi.org/10.1038/347563a0

Hagan, I., and M. Yanagida. 1992. Kinesin-related cut7 protein associates with mitotic and meiotic spindles in fission yeast. *Nature*. 356:74–76. http://dx.doi.org/10.1038/356074a0

Heck, M.M., A. Pereira, P. Pesavento, Y. Yannoni, A.C. Spradling, and L.S. Goldstein. 1993. The kinesin-like protein KLP61F is essential for mitosis in *Drosophila*. *J. Cell Biol.* 123:665–679. http://dx.doi.org/10.1083/jcb.123.3.665

Hentrich, C., and T. Surrey. 2010. Microtubule organization by the antagonistic mitotic motors kinesin-5 and kinesin-14. *J. Cell Biol.* 189:465–480. http://dx.doi.org/10.1083/jcb.200910125

Hiraoka, Y., T. Toda, and M. Yanagida. 1984. The *NDA3* gene of fission yeast encodes β-tubulin: a cold-sensitive *nda3* mutation reversibly blocks spindle formation and chromosome movement in mitosis. *Cell*. 39:349–358. http://dx.doi.org/10.1016/0092-8674(84)90013-8

Hori, A., C. Ikebe, M. Tada, and T. Toda. 2014. Msd1/SSX2IP-dependent microtubule anchorage ensures spindle orientation and primary cilia formation. *EMBO Rep.* 15:175–184.

Hoyt, M.A., L. He, K.K. Loo, and W.S. Saunders. 1992. Two *Saccharomyces cerevisiae* kinesin-related gene products required for mitotic spindle assembly. *J. Cell Biol.* 118:109–120. http://dx.doi.org/10.1083/jcb.118.1.109

Hutchins, J.R., Y. Toyoda, B. Hegemann, I. Poser, J.K. Hériché, M.M. Sykora, M. Augsburg, O. Hudecz, B.A. Buschhorn, J. Bulkescher, et al. 2010. Systematic analysis of human protein complexes identifies chromosome segregation proteins. *Science*. 328:593–599. http://dx.doi.org/10.1126/science.1181348

Ikebe, C., M. Konishi, D. Hirata, T. Matsusaka, and T. Toda. 2011. Systematic localization study on novel proteins encoded by meiotically up-regulated ORFs in fission yeast. *Biosci. Biotechnol. Biochem.* 75:2364–2370. http://dx.doi.org/10.1271/bbb.110558

Jakobsen, L., K. Vanselow, M. Skogs, Y. Toyoda, E. Lundberg, I. Poser, L.G. Falkenby, M. Bennetzen, J. Westendorf, E.A. Nigg, et al. 2011. Novel asymmetrically localizing components of human centrosomes identified by complementary proteomics methods. *EMBO J.* 30:1520–1535. http://dx.doi.org/10.1038/emboj.2011.63

Kalderon, D., B.L. Roberts, W.D. Richardson, and A.E. Smith. 1984. A short amino acid sequence able to specify nuclear location. *Cell*. 39:499–509. http://dx.doi.org/10.1016/0092-8674(84)90457-4

Kapitein, L.C., E.J. Peterman, B.H. Kwok, J.H. Kim, T.M. Kapoor, and C.F. Schmidt. 2005. The bipolar mitotic kinesin Eg5 moves on both microtubules that it crosslinks. *Nature*. 435:114–118. http://dx.doi.org/10.1038/nature03503

Kashina, A.S., R.J. Baskin, D.G. Cole, K.P. Wedaman, W.M. Saxton, and J.M. Scholey. 1996. A bipolar kinesin. *Nature*. 379:270–272. http://dx.doi.org/10.1038/379270a0

Klinger, M., W. Wang, S. Kuhns, F. Bärenz, S. Dräger-Meurer, G. Pereira, and O.J. Gruss. 2014. The novel centriolar satellite protein SSX2IP targets Cep290 to the ciliary transition zone. *Mol. Biol. Cell*. 25:495–507. http://dx.doi.org/10.1091/mbc.E13-09-0526

Kollman, J.M., A. Merdes, L. Mourey, and D.A. Agard. 2011. Microtubule nucleation by γ-tubulin complexes. *Nat. Rev. Mol. Cell Biol.* 12:709–721. http://dx.doi.org/10.1038/nrm3209

Koshizuka, Y., S. Ikegawa, M. Sano, K. Nakamura, and Y. Nakamura. 2001. Isolation, characterization, and mapping of the mouse and human *WDR8* genes, members of a novel WD-repeat gene family. *Genomics*. 72:252–259. http://dx.doi.org/10.1006/geno.2000.6475

Kwon, M., S.A. Godinho, N.S. Chandhok, N.J. Ganem, A. Azioune, M. Thery, and D. Pellman. 2008. Mechanisms to suppress multipolar divisions in cancer cells with extra centrosomes. *Genes Dev.* 22:2189–2203. http://dx.doi.org/10.1101/gad.1700908

Lawrence, C.J., R.K. Dawe, K.R. Christie, D.W. Cleveland, S.C. Dawson, S.A. Endow, L.S. Goldstein, H.V. Goodson, N. Hirokawa, J. Howard, et al. 2004. A standardized kinesin nomenclature. *J. Cell Biol.* 167:19–22. http://dx.doi.org/10.1083/jcb.200408113

Lecland, N., and J. Lüders. 2014. The dynamics of microtubule minus ends in the human mitotic spindle. *Nat. Cell Biol.* 16:770–778. http://dx.doi.org/10.1038/ncb2996

Lin, T.C., A. Neuner, Y.T. Schlosser, A.N. Scharf, L. Weber, and E. Schiebel. 2014. Cell-cycle dependent phosphorylation of yeast pericentrin regulates γ-TuSC-mediated microtubule nucleation. *eLife*. 3:e02208. http://dx.doi.org/10.7554/eLife.02208

Lüders, J., and T. Stearns. 2007. Microtubule-organizing centres: a re-evaluation. *Nat. Rev. Mol. Cell Biol.* 8:161–167. http://dx.doi.org/10.1038/nrm2100

Mahmoudi, S., S. Henriksson, M. Corcoran, C. Méndez-Vidal, K.G. Wiman, and M. Farnebo. 2009. Wrap53, a natural p53 antisense transcript required for p53 induction upon DNA damage. *Mol. Cell*. 33:462–471. http://dx.doi.org/10.1016/j.molcel.2009.01.028

Masuda, H., R. Mori, M. Yukawa, and T. Toda. 2013. Fission yeast MOZART1/Mzt1 is an essential γ-tubulin complex component required for complex recruitment to the microtubule organizing center, but not its assembly. *Mol. Biol. Cell*. 24:2894–2906. http://dx.doi.org/10.1091/mbc.E13-05-0235

Mayer, T.U., T.M. Kapoor, S.J. Haggarty, R.W. King, S.L. Schreiber, and T.J. Mitchison. 1999. Small molecule inhibitor of mitotic spindle bipolarity identified in a phenotype-based screen. *Science*. 286:971–974. http://dx.doi.org/10.1126/science.286.5441.971

Meluh, P.B., and M.D. Rose. 1990. KAR3, a kinesin-related gene required for yeast nuclear fusion. *Cell*. 60:1029–1041. http://dx.doi.org/10.1016/0092-8674(90)90351-E

Mennella, V., D.A. Agard, B. Huang, and L. Pelletier. 2014. Amorphous no more: subdiffraction view of the pericentriolar material architecture. *Trends Cell Biol.* 24:188–197. http://dx.doi.org/10.1016/j.tcb.2013.10.001

Meunier, S., and I. Vernos. 2012. Microtubule assembly during mitosis - from distinct origins to distinct functions? *J. Cell Sci.* 125:2805–2814. http://dx.doi.org/10.1242/jcs.092429

Miki, F., K. Okazaki, M. Shimanuki, A. Yamamoto, Y. Hiraoka, and O. Niwa. 2002. The 14-kDa dynein light chain-family protein Dlc1 is required for regular oscillatory nuclear movement and efficient recombination during meiotic prophase in fission yeast. *Mol. Biol. Cell*. 13:930–946. http://dx.doi.org/10.1091/mbc.01-11-0543

Moreno, S., A. Klar, and P. Nurse. 1991. Molecular genetic analysis of fission yeast *Schizosaccharomyces pombe*. *Methods Enzymol.* 194:795–823. http://dx.doi.org/10.1016/0076-6879(91)94059-L

Mountain, V., C. Simerly, L. Howard, A. Ando, G. Schatten, and D.A. Compton. 1999. The kinesin-related protein, HSET, opposes the activity of Eg5 and cross-links microtubules in the mammalian mitotic spindle. *J. Cell Biol.* 147:351–366. http://dx.doi.org/10.1083/jcb.147.2.351

Mulvihill, D.P., J. Petersen, H. Ohkura, D.M. Glover, and I.M. Hagan. 1999. Plo1 kinase recruitment to the spindle pole body and its role in cell division in *Schizosaccharomyces pombe*. *Mol. Biol. Cell*. 10:2771–2785. http://dx.doi.org/10.1091/mbc.10.8.2771

Niwa, O., T. Matsumoto, Y. Chikashige, and M. Yanagida. 1989. Characterization of *Schizosaccharomyces pombe* minichromosome deletion derivatives and a functional allocation of their centromere. *EMBO J.* 8:3045–3052.

O'Connell, M.J., P.B. Meluh, M.D. Rose, and N.R. Morris. 1993. Suppression of the *bimC4* mitotic spindle defect by deletion of *klpA*, a gene encoding a KAR3-related kinesin-like protein in *Aspergillus nidulans*. *J. Cell Biol.* 120:153–162. http://dx.doi.org/10.1083/jcb.120.1.153

Olmsted, Z.T., T.D. Riehlman, C.N. Branca, A.G. Colliver, L.O. Cruz, and J.L. Paluh. 2013. Kinesin-14 Pkl1 targets γ-tubulin for release from the γ-tubulin ring complex (γ-TuRC). *Cell Cycle*. 12:842–848. http://dx.doi.org/10.4161/cc.23822

Olmsted, Z.T., A.G. Colliver, T.D. Riehlman, and J.L. Paluh. 2014. Kinesin-14 and kinesin-5 antagonistically regulate microtubule nucleation by γ-TuRC in yeast and human cells. *Nat. Commun.* 5:5339. http://dx.doi.org/10.1038/ncomms6339

Osmani, A.H., J. Davies, C.E. Oakley, B.R. Oakley, and S.A. Osmani. 2003. TINA interacts with the NIMA kinase in *Aspergillus nidulans* and negatively regulates astral microtubules during metaphase arrest. *Mol. Biol. Cell*. 14:3169–3179. http://dx.doi.org/10.1091/mbc.E02-11-0715

Paluh, J.L., E. Nogales, B.R. Oakley, K. McDonald, A.L. Pidoux, and W.Z. Cande. 2000. A mutation in γ-tubulin alters microtubule dynamics and organization and is synthetically lethal with the kinesin-like protein pkl1p. *Mol. Biol. Cell*. 11:1225–1239. http://dx.doi.org/10.1091/mbc.11.4.1225

Pickett-Heaps, J.D. 1969. The evolution of the mitotic apparatus: an attempt at comparative ultrastructural cytology in dividing plant cells. *Cytobios*. 3: 257–280.

Pidoux, A.L., M. LeDizet, and W.Z. Cande. 1996. Fission yeast pkl1 is a kinesin-related protein involved in mitotic spindle function. *Mol. Biol. Cell*. 7:1639–1655. http://dx.doi.org/10.1091/mbc.7.10.1639

Rodriguez, A.S., J. Batac, A.N. Killilea, J. Filopei, D.R. Simeonov, I. Lin, and J.L. Paluh. 2008. Protein complexes at the microtubule organizing center regulate bipolar spindle assembly. *Cell Cycle*. 7:1246–1253. http://dx.doi.org/10.4161/cc.7.9.5808

Roof, D.M., P.B. Meluh, and M.D. Rose. 1992. Kinesin-related proteins required for assembly of the mitotic spindle. *J. Cell Biol.* 118:95–108. http://dx.doi.org/10.1083/jcb.118.1.95

Roostalu, J., C. Hentrich, P. Bieling, I.A. Telley, E. Schiebel, and T. Surrey. 2011. Directional switching of the kinesin Cin8 through motor coupling. *Science*. 332:94–99. http://dx.doi.org/10.1126/science.1199945

Rothbauer, U., K. Zolghadr, S. Muyldermans, A. Schepers, M.C. Cardoso, and H. Leonhardt. 2008. A versatile nanotrap for biochemical and functional studies with fluorescent fusion proteins. *Mol. Cell. Proteomics*. 7:282–289. http://dx.doi.org/10.1074/mcp.M700342-MCP200

Salemi, J.D., P.T. McGilvray, and T.J. Maresca. 2013. Development of a *Drosophila* cell-based error correction assay. *Front Oncol*. 3:187. http://dx.doi.org/10.3389/fonc.2013.00187

Sato, M., S. Dhut, and T. Toda. 2005. New drug-resistant cassettes for gene disruption and epitope tagging in *Schizosaccharomyces pombe*. *Yeast*. 22:583–591. http://dx.doi.org/10.1002/yea.1233

Saunders, W.S., and M.A. Hoyt. 1992. Kinesin-related proteins required for structural integrity of the mitotic spindle. *Cell*. 70:451–458. http://dx.doi.org/10.1016/0092-8674(92)90169-D

Saunders, W., V. Lengyel, and M.A. Hoyt. 1997. Mitotic spindle function in *Saccharomyces cerevisiae* requires a balance between different types of kinesin-related motors. *Mol. Biol. Cell*. 8:1025–1033. http://dx.doi.org/10.1091/mbc.8.6.1025

Sharp, D.J., K.L. McDonald, H.M. Brown, H.J. Matthies, C. Walczak, R.D. Vale, T.J. Mitchison, and J.M. Scholey. 1999. The bipolar kinesin, KLP61F, cross-links microtubules within interpolar microtubule bundles of *Drosophila* embryonic mitotic spindles. *J. Cell Biol.* 144:125–138. http://dx.doi.org/10.1083/jcb.144.1.125

Sharp, D.J., G.C. Rogers, and J.M. Scholey. 2000. Microtubule motors in mitosis. *Nature*. 407:41–47. http://dx.doi.org/10.1038/35024000

Shen, K.F., and S.A. Osmani. 2013. Regulation of mitosis by the NIMA kinase involves TINA and its newly discovered partner, An-WDR8, at spindle pole bodies. *Mol. Biol. Cell*. 24:3842–3856. http://dx.doi.org/10.1091/mbc.E13-07-0422

Tanenbaum, M.E., and R.H. Medema. 2010. Mechanisms of centrosome separation and bipolar spindle assembly. *Dev. Cell*. 19:797–806. http://dx.doi.org/10.1016/j.devcel.2010.11.011

Tao, L., A. Mogilner, G. Civelekoglu-Scholey, R. Wollman, J. Evans, H. Stahlberg, and J.M. Scholey. 2006. A homotetrameric kinesin-5, KLP61F, bundles microtubules and antagonizes Ncd in motility assays. *Curr. Biol.* 16:2293–2302. http://dx.doi.org/10.1016/j.cub.2006.09.064

Toya, M., M. Sato, U. Haselmann, K. Asakawa, D. Brunner, C. Antony, and T. Toda. 2007. γ-tubulin complex-mediated anchoring of spindle microtubules to spindle-pole bodies requires Msd1 in fission yeast. *Nat. Cell Biol.* 9:646–653. http://dx.doi.org/10.1038/ncb1593

Troxell, C.L., M.A. Sweezy, R.R. West, K.D. Reed, B.D. Carson, A.L. Pidoux, W.Z. Cande, and J.R. McIntosh. 2001. *pkl1(+)* and *klp2(+)*: Two kinesins of the Kar3 subfamily in fission yeast perform different functions in both mitosis and meiosis. *Mol. Biol. Cell*. 12:3476–3488. http://dx.doi.org/10.1091/mbc.12.11.3476

Vardy, L., and T. Toda. 2000. The fission yeast γ-tubulin complex is required in $G_{(1)}$ phase and is a component of the spindle assembly checkpoint. *EMBO J.* 19:6098–6111. http://dx.doi.org/10.1093/emboj/19.22.6098

Venkatram, S., J.J. Tasto, A. Feoktistova, J.L. Jennings, A.J. Link, and K.L. Gould. 2004. Identification and characterization of two novel proteins affecting fission yeast γ-tubulin complex function. *Mol. Biol. Cell*. 15:2287–2301. http://dx.doi.org/10.1091/mbc.E03-10-0728

Walczak, C.E., I. Vernos, T.J. Mitchison, E. Karsenti, and R. Heald. 1998. A model for the proposed roles of different microtubule-based motor proteins in establishing spindle bipolarity. *Curr. Biol.* 8:903–913. http://dx.doi.org/10.1016/S0960-9822(07)00370-3

West, R.R., E.V. Vaisberg, R. Ding, P. Nurse, and J.R. McIntosh. 1998. *cut11(+)*: A gene required for cell cycle-dependent spindle pole body anchoring in the nuclear envelope and bipolar spindle formation in *Schizosaccharomyces pombe*. *Mol. Biol. Cell*. 9:2839–2855. http://dx.doi.org/10.1091/mbc.9.10.2839

Wittmann, T., A. Hyman, and A. Desai. 2001. The spindle: a dynamic assembly of microtubules and motors. *Nat. Cell Biol.* 3:E28–E34. http://dx.doi.org/10.1038/35050669

Yamamoto, A., R.R. West, J.R. McIntosh, and Y. Hiraoka. 1999. A cytoplasmic dynein heavy chain is required for oscillatory nuclear movement of meiotic prophase and efficient meiotic recombination in fission yeast. *J. Cell Biol.* 145:1233–1249. http://dx.doi.org/10.1083/jcb.145.6.1233